

Finite-Bit Quantization For Distributed Algorithms With Linear Convergence

Chang-Shen Lee, Nicolò Michelusi, and Gesualdo Scutari

Abstract

This paper studies distributed algorithms for (strongly convex) composite optimization problems over mesh networks, subject to quantized communications. Instead of focusing on a specific algorithmic design, we propose a black-box model casting distributed algorithms in the form of fixed-point iterates, converging at linear rate. The algorithmic model is coupled with a novel (random) Biased Compression (BC-)rule on the quantizer design, which preserves *linear* convergence. A new quantizer coupled with a communication-efficient encoding scheme is also proposed, which efficiently implements the BC-rule using a *finite* number of bits. This contrasts with most of existing quantization rules, whose implementation calls for an *infinite* number of bits. A unified communication complexity analysis is developed for the black-box model, determining the average number of bit required to reach a solution of the optimization problem within the required accuracy. Numerical results validate our theoretical findings and show that distributed algorithms equipped with the proposed quantizer have more favorable communication complexity than algorithms using existing quantization rules.

I. INTRODUCTION

We study distributed optimization over a network of m agents modeled as an undirected (connected) graph. We consider mesh networks, that is, arbitrary topologies with no central hub connected to all the other agents, where each agent can communicate with its immediate

C.-S. Lee is with the School of Electrical and Computer Engineering, Purdue University, IN, USA; email: lee2495@purdue.edu.

N. Michelusi is with the School of Electrical, Computer and Energy Engineering, Arizona State University, AZ, USA; email: nicolo.michelusi@asu.edu.

G. Scutari is with the School of Industrial Engineering, Purdue University, IN, USA; email: gscutari@purdue.edu.

The work of Lee and Scutari was partially supported by the National Science Foundation under the grant CIF 1719205; the Army Research Office under the grant W911NF1810238; and the Office of Naval Research, under the grant N00014-21-1-2673. Michelusi's work was supported in part by the National Science Foundation under grants CNS-1642982 and CNS-2129015.

arXiv:2107.11304v1 [math.OC] 23 Jul 2021

neighbors (master/worker architectures will be treated as a special case). The m agents aim at solving cooperatively the optimization problem

$$\min_{\mathbf{x} \in \mathbb{R}^d} \underbrace{\frac{1}{m} \sum_{i=1}^m f_i(\mathbf{x})}_{=F(\mathbf{x})} + r(\mathbf{x}), \quad (\text{P})$$

where each f_i is the local cost function of agent i , assumed to be smooth, convex, and known only to the agent; $r : \mathbb{R}^d \rightarrow [-\infty, \infty]$ is a nonsmooth, convex (extended-value) function known to all agents, which can be used to force shared constraints or some structure on the solution (e.g., sparsity); and the global loss $F : \mathbb{R}^d \rightarrow \mathbb{R}$ is assumed to be strongly convex on the domain of r . This setting is fairly general and finds applications in several areas, including network information processing, telecommunications, multi-agent control, and machine learning (e.g., [1]–[3]).

Since the functions f_i can be accessed only locally and routing local data to other agents is infeasible or highly inefficient, solving (P) calls for the design of distributed algorithms that alternate between a local computation procedure at each agent’s side and some rounds of communication among neighboring nodes. While most existing works focus on *ad-hoc* solution methods, here we consider a *general* distributed algorithmic framework, encompassing algorithms whose dynamics are modeled by the fixed-point iteration

$$\mathbf{z}^{k+1} = \tilde{\mathcal{A}}(\mathbf{z}^k), \quad (1)$$

where \mathbf{z}^k is the updating variable at iteration k and $\tilde{\mathcal{A}}$ is a mapping that embeds the local computation and communication steps, whose fixed point typically coincides with the solutions of (P). This model encompasses several distributed algorithms over different network architectures, each one corresponding to a specific expression of \mathbf{z} and $\tilde{\mathcal{A}}$ —see Sec. II for some examples.

By assuming that F is strongly convex, with (1) we explicitly target distributed schemes converging to solutions of (P) at *linear rate*. Furthermore, since the cost of communications is often the bottleneck for distributed computing when compared with local (possibly parallel) computations (e.g., [4], [5]), we achieve communication efficiency by embedding the iterates (1) with quantized communication protocols. Our goal is to design a black-box quantization mechanism for the class of distributed algorithms (1) that preserves their linear convergence while employing *finite-bit* quantized communications.

To our knowledge, this is an open problem, since there exists no *linearly* convergent distributed algorithmic *framework* for the general class of the composite (constrained) optimization problems

(P) employing *finite-bit* communications. While we defer to Sec. I-B for a detailed literature review, here we only point out that existing distributed schemes employing some form of quantization of the communications are applicable only to smooth, unconstrained instances of (P) (i.e., $r = 0$) [6]–[14]. Furthermore, the majority of such algorithms require *infinite-bit* communications [6]–[11]. The exceptions are [12], [13] and our work [14]; yet, the quantization schemes developed in these papers are tailored to a specific distributed algorithm, namely, a primal-dual scheme in [12] and NEXT [15]–[17] in [13], [14].

A. Summary of main contributions

Our major contributions are summarized next—see also Table I.

- **A black-box quantization model for (1):** We propose a novel black-box model that introduces quantization in the communication steps of all distributed algorithms cast in the form (1). Our approach paves the way to a *unified* design of quantization rules and analysis of their impact on the convergence rate of a gamut of distributed algorithms. This constitutes a major departure from the majority of existing studies focusing on ad-hoc algorithms and quantization rules, which in fact are special instances of our framework. Furthermore, our model brings for the first time quantization to distributed algorithms applicable to composite optimization (P) (i.e., with $r \neq 0$).
- **Preserving linear convergence of (1) under quantization:** We provide a novel *biased compression* rule (the BC-rule) on the quantizer design equipping the proposed black-box model, which preserves *linear* convergence of the distributed algorithms while using a *finite* number of bits and *without* altering their original tuning. Our condition encompasses several deterministic and random quantization rules, new and old [12]–[14], [18]–[31]. Furthermore, our analysis reveals that, despite common wisdom, several rules proposed in the literature for signal compression and used in particular for quantization [6]–[11], [32]–[41] cannot be implemented using a finite number of bits.
- **A novel finite-bit quantizer:** To make the BC-rule practical, we also propose a novel *finite-bit* quantizer fulfilling the BC-rule along with a communication-efficient bit-encoding/decoding rule which enables transmissions on digital channels; it is termed *Adaptive encoding Nonuniform Quantization* (ANQ). ANQ is a deterministic quantizer that adapts the number of bits of the output (discrete representation) based upon the input signal. By doing so, it achieves a more communication-efficient design than existing quantizers that encode the signal by using a fixed

number of bits based on the worst-case range of the input signal (a predetermined fixed range in [18]–[21], [23], [24], [26], [27], [29]–[31], or a shrinking one in [12]–[14], [22], [25], [28]).

• **Communication complexity:** We derive the first communication complexity for quantized distributed algorithms over *mesh networks* (see. Table I), in terms of average number of bits required to reach an ε -solution of (P) (using a proper optimality measure—see Theorem 13) by *any* distributed algorithm belonging to our black-box model. This also sheds light on the dependence of the convergence rate and communication cost on the quantization design parameters.

Finally, we validate numerically our theoretical findings on regularized least square and logistic regression problems. Among others, our evaluations show that 1) linear convergence of all distributed algorithms is preserved under finite-bit quantization based upon the proposed BC-rule; as predicted by our analysis, the rate approaches the one of their unquantized counterpart scheme when a sufficient number of bits is used; 2) the proposed ANQ rule outperforms existing finite-bit quantization rules; and 3) a benchmark of several distributed schemes under quantization is provided, for which convergence guarantees are established for the first time in this work.

B. Related works

The literature on distributed algorithms is vast; here, we review relevant works employing some form of quantization with linear convergence guarantees [6]–[10], [12]–[14], categorized into those requiring infinite or finite number of bits.

1) Infinite-bit quantization schemes [6]–[10]: Distributed algorithms employing quantization in the agents’ communications are proposed in [6]–[10] for special instances of (P) with $r = 0$ (i.e., smooth and unconstrained optimization). In these schemes, quantization is implemented by compressing the signal $\mathbf{x} \in \mathbb{R}^d$ through a (random or deterministic¹) *compression operator* $\mathbf{x} \mapsto \mathcal{Q}(\mathbf{x})$, that satisfies the *compression rule*

$$\sqrt{\mathbb{E}[\|\mathcal{Q}(\mathbf{x}) - \mathbf{x}\|_2^2]} \leq \omega \|\mathbf{x}\|_2, \quad \text{for some } \omega \in (0, 1). \quad (2)$$

Despite common wisdom, we prove that all the quantization rules derived from (2)—hence those in [6]–[10]—can only be implemented using an *infinite* number of bits (see Corollary 9). This calls for the development of new compression rules using a finite number of bits. The proposed BC-rule provides a positive answer to this question.

¹We treat compression rules using deterministic mappings \mathcal{Q}^k as special cases of the random ones; in this case, the expected value operator will just return the deterministic value argument.

2) Finite-bit quantization schemes [12]–[14]: While finite-rate quantization has been extensively studied for average consensus schemes (e.g., [19], [20], [22], [23], [25], [28]–[31]), their extension to optimization algorithms over mesh networks is less explored [12]–[14]. Specifically, in our conference work [14], we equip the NEXT algorithm [15], [16] with a finite-bit deterministic quantization to solve (P) with $r = 0$; to preserve linear convergence, the quantizer shrinks its input range linearly. An expression of the convergence rate of the scheme in [14] has been later determined in [13] along with its scaling properties with respect to problem, network, and quantization parameters.

The closest paper to our work is [12], where the authors proposed a finite-bit quantization mechanism preserving linear convergence of a sub-class of algorithms cast as (1). Yet, there are several key differences between [12] and our work. First, the convergence analysis in [12] is applicable only to algorithms solving smooth, unconstrained optimization problems, and thus not to Problem (P) with $r \neq 0$. Second, linear convergence under finite-bit quantization is explicitly proved in [12] only for schemes whose updates utilize current iterate information, namely: gradient descent (GD) over star networks and the primal-dual algorithm in [42] over mesh networks. This leaves open the question whether distributed algorithms using historical information—e.g., in the form of gradient tracking or dual variables—are linearly convergent under finite-bit quantization, and under which conditions; renowned examples include EXTRA [43], AugDGM [44], DIGing [45], Harnessing [46], and NEXT [15], [16]. Our work provides a positive answer to these open questions. Third, communication complexity of the scheme in [12] is not provided over mesh networks, which instead is a novel contribution of this work for a wide class of distributed algorithms—see Table I and Sec. V. Fourth, [12] proposed an ad-hoc deterministic quantization rule while the proposed BC-rule encompasses several deterministic and random quantizations (including that in [12] as a special case), possibly using a variable number of bits (adapted to the input signal). As a result, even when customized to the setting/algorithms in [12], the BC-rule leads to more communication-efficient schemes, both analytically (see Sec. V) and numerically (see Sec. VI)—see also Table I.

C. Organization and notation

The remainder of this paper is organized as follows. Sec. II introduces the proposed black-box model for casting distributed algorithms in the form (1). Sec. III embeds quantized communications, introduces the proposed BC-rule, and analyzes the convergence properties. Sec. IV

Ref.	Problem	# of bits/agent to ε accuracy	Algorithms
[14]	(P) with $r = 0$	N/A	ad-hoc (NEXT [15], [16])
[13]	(P) with $r = 0$	N/A	ad-hoc (NEXT [15], [16])
[12]	(P) with $r = 0$	$\mathcal{O}\left(\log_2\left(1 + \frac{d}{1-\lambda}\right) \frac{d}{1-\lambda} \log_2(d/\varepsilon)\right)$	GD over star networks
		N/A	ad-hoc (primal-dual [42])
This paper	(P)	$\mathcal{O}\left(\log_2\left(1 + \frac{1}{1-\lambda}\right) \frac{d}{1-\lambda} \log_2(d/\varepsilon)\right)$	All the schemes listed in the caption of the table

TABLE I: Comparison with the state-of-the-art distributed algorithms using some form of quantization; λ is the convergence rate of the input (unquantized) algorithm, and d is the dimension of \mathbf{x} . The scheme proposed in this paper is applicable to the distributed algorithms listed in the table and, in addition, to the following: general primal-dual-based methods [47], EXTRA [43], NEXT [15], [16], AugDGM [48], DIGing [45], the scheme in [46], NIDS [49], Exact Diffusion [50], and some of their proximal counterpart as those in [51] and [47].

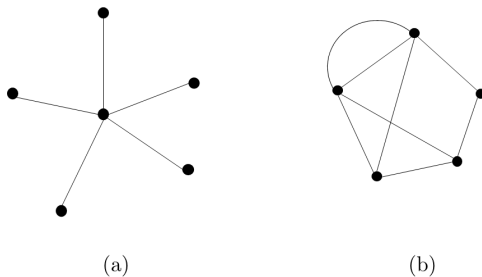


Fig. 1: Examples of star network (a) versus mesh topology (b).

describes the proposed quantizer, the ANQ, and studies communication complexity. Sec. V customizes the proposed framework and convergence guarantees to several existing distributed algorithms, equipping them with the ANQ rule. Sec. VI provides some numerical results, while Sec. VII draws some conclusions. All the proofs of our results are presented in the appendix.

Notation: Throughout the paper, we will use the following notation. We denote by \mathbb{Z}, \mathbb{R} the set of integers and real numbers, respectively. For any positive integer a , we define $[a] \triangleq \{1, \dots, a\}$. We denote by $\mathbf{0}, \mathbf{1}$, and \mathbf{I} the vector of all zeros, the vector of all ones, and the identity matrix, respectively. For vectors $\mathbf{c}_1, \dots, \mathbf{c}_m$ and a set $\mathcal{S} \subseteq [m]$, define $\mathbf{c}_{\mathcal{S}} \triangleq \{\mathbf{c}_i : i \in \mathcal{S}\}$. We use $\|\cdot\|$ to denote a norm in the Euclidean space (whose dimension will be clear from the context); when a specific norm is used, such as ℓ_2 or ℓ_∞ , we will append the associated subscript to $\|\cdot\|$. The i th eigenvalue of a real, symmetric matrix \mathbf{G} is denoted by $\rho_i(\mathbf{G})$, ordered in nonincreasing order such that $\rho_1(\mathbf{G}) \geq \dots \geq \rho_i(\mathbf{G}) \geq \rho_{i+1}(\mathbf{G})$. We will use a superscript to denote iteration counters of sequences generated by the algorithms, for instance, x^k will denote the value of the x -sequence at iteration k . We will instead use $(x)^k$ for the k -power of x . Finally, asymptotic behaviors

of functions are captured by the standard big- \mathcal{O} , Θ , and Ω notations: 1) $g(x) = \mathcal{O}(h(x))$ as $x \rightarrow x_0$ iff. $\limsup_{x \rightarrow x_0} |g(x)/h(x)| \in [0, \infty)$; 2) $g(x) = \Omega(h(x))$ iff. $h(x) = \mathcal{O}(g(x))$; and 3) $g(x) = \Theta(h(x))$ iff. $g(x) = \mathcal{O}(h(x)) = \Omega(h(x))$.

We model a network of m agents as a fixed, undirected, connected graph $\mathcal{G} = (\mathcal{V}, \mathcal{E})$, where $\mathcal{V} = [m]$ is the set of vertices (agents) and $\mathcal{E} \subseteq \mathcal{V} \times \mathcal{V}$ is the set of edges (communication links); $(i, j) \in \mathcal{E}$ if there is a link between agents i and j , so that the two can send information to each other. We let $\mathcal{N}_i = \{j : (i, j) \in \mathcal{E}\}$ be the set of neighbors of agent i , and assume that $(i, i) \in \mathcal{E}$, i.e., $i \in \mathcal{N}_i$. Master/workers architectures will be considered as special cases—see Fig. 1.

II. A GENERAL DISTRIBUTED ALGORITHMIC FRAMEWORK: EXACT COMMUNICATIONS

In this section, we show how to cast distributed algorithms for (P) in the form (1). As a warm-up, we begin with schemes using only current information to produce the next update (cf. Sec. II-A). We then generalize the model to capture distributed algorithms using historical information via multiple rounds of communications between computation steps (cf. Sec. II-B).

A. Warm-up: A class of distributed algorithms

We cast distributed algorithms in the form (1) by incorporating computations and communications as two separate steps. We use state variable \mathbf{z}_i to capture local information owned by agent i (including optimization variables) and $\hat{\mathbf{c}}_i$ to denote the signal transmitted by agent i to its neighbors.² Similarly to [12], the updates of the \mathbf{z} , $\hat{\mathbf{c}}$ -variables read: for agent $i \in [m]$,

$$\begin{aligned} \hat{\mathbf{c}}_i^k &= \mathcal{C}_i(\mathbf{z}_i^k), & (\text{communication step}) \\ \mathbf{z}_i^{k+1} &= \mathcal{A}_i(\mathbf{z}_i^k, \hat{\mathbf{c}}_{\mathcal{N}_i}^k), & (\text{computation step}) \end{aligned} \tag{M0}$$

where the function $\mathbf{z}_i \mapsto \mathcal{C}_i(\mathbf{z}_i)$ models the processing on the local information \mathbf{z}_i^k at the current iterate, generating the signal $\hat{\mathbf{c}}_i^k$ to be transmitted to agent i 's neighbors; and the function $(\mathbf{z}_i, \hat{\mathbf{c}}_{\mathcal{N}_i}) \mapsto \mathcal{A}_i(\mathbf{z}_i, \hat{\mathbf{c}}_{\mathcal{N}_i})$ is the function producing the update of the agent i 's state variable \mathbf{z}_i , based upon the local information at iteration k (including the signals received by its neighbors).

Some examples: The algorithmic model (M0) captures a variety of distributed algorithms that build updates using single rounds of communications; examples include the renewed DGD [52],

²Dimensions of these vectors are algorithm-dependent and omitted for simplicity, and will be clear from the context.

NIDS [49], and the primal-dual scheme [42]. To show a concrete example, consider DGD, which aims at solving a special instance of (P) with $r = 0$; agents' updates read

$$\mathbf{x}_i^{k+1} = \left(\sum_{j=1}^m w_{ij} \mathbf{x}_j^k \right) - \gamma \nabla f_i(\mathbf{x}_i^k), \quad i \in [m],$$

where \mathbf{x}_i^k is the local copy owned by agent i at iteration k of the optimization variables \mathbf{x} , γ is a step-size, and w_{ij} 's are nonnegative weights properly chosen and compliant with the graph \mathcal{G} (i.e., $w_{ij} > 0$ if $(i, j) \in \mathcal{E}$; and $w_{ij} = 0$ otherwise). It is not difficult to check that DGD can be rewritten in the form (M0) by letting

$$\mathbf{z}_i^k = \hat{\mathbf{c}}_i^k = \mathbf{x}_i^k \quad \text{and} \quad \mathcal{A}_i(\mathbf{z}_i^k, \hat{\mathbf{c}}_{\mathcal{N}_i}^k) = \left(\sum_{j=1}^m w_{ij} \hat{\mathbf{c}}_j^k \right) - \gamma \nabla f_i(\mathbf{z}_i^k).$$

Despite its generality, model (M0) leaves out several important distributed algorithms, specifically, the majority of schemes employing correction of the gradient direction based on past state information—these are the best performing algorithms to date. Examples include EXTRA [43], DIGing [45] and their proximal version, NEXT/SONATA [15]–[17], and the ABC framework [47], just to name a few. Consider for instance NEXT/SONATA:

$$\mathbf{x}_i^{k+1} = \sum_{j \in \mathcal{N}_i} w_{ij} (\mathbf{x}_j^k - \gamma \mathbf{y}_j^k) \quad \text{and} \quad \mathbf{y}_i^{k+1} = \sum_{j \in \mathcal{N}_i} w_{ij} (\mathbf{y}_j^k + \nabla f_j(\mathbf{x}_j^{k+1}) - \nabla f_j(\mathbf{x}_j^k)). \quad (3)$$

Clearly, this does not fit model (M0): the update of the y -variable uses information from two iteration ages (k and $k + 1$). This calls for a more general model, introduced next.

B. Proposed general model (using historical information)

We generalize the algorithmic model (M0) as follows: for all $i \in [m]$,

$$\left. \begin{aligned} \hat{\mathbf{c}}_i^{k,1} &= \mathcal{C}_i^1(\mathbf{z}_i^k, \mathbf{0}_{\mathcal{N}_i}), \\ &\vdots \\ \hat{\mathbf{c}}_i^{k,R} &= \mathcal{C}_i^R(\mathbf{z}_i^k, \hat{\mathbf{c}}_{\mathcal{N}_i}^{k,R-1}), \end{aligned} \right\} \text{(multiple communication rounds)} \quad (\text{M})$$

$$\mathbf{z}_i^{k+1} = \mathcal{A}_i(\mathbf{z}_i^k, \hat{\mathbf{c}}_{\mathcal{N}_i}^{k,1}, \dots, \hat{\mathbf{c}}_{\mathcal{N}_i}^{k,R}), \quad \text{(computation step)}$$

which embeds $R \geq 1$ rounds of local communications, via the functions $(\mathbf{z}_i, \hat{\mathbf{c}}_{\mathcal{N}_i}^{s-1}) \mapsto \mathcal{C}_i^s(\mathbf{z}_i, \hat{\mathbf{c}}_{\mathcal{N}_i}^{s-1})$; and the function $(\mathbf{z}_i, \hat{\mathbf{c}}_{\mathcal{N}_i}^1, \dots, \hat{\mathbf{c}}_{\mathcal{N}_i}^R) \mapsto \mathcal{A}_i(\mathbf{z}_i, \hat{\mathbf{c}}_{\mathcal{N}_i}^1, \dots, \hat{\mathbf{c}}_{\mathcal{N}_i}^R)$ updates the local state by possibly using the signals $\hat{\mathbf{c}}_{\mathcal{N}_i}$'s received from all neighbors during all R rounds of communications,

along with \mathbf{z}_i . Stacking agents' state-variables \mathbf{z}_i , communication signals $\hat{\mathbf{c}}_i$, and mappings \mathcal{C}_i^s and \mathcal{A}_i into the respective vectors \mathbf{z} , $\hat{\mathbf{c}}$, \mathcal{C}^s and \mathcal{A} , we can rewrite (M) in compact form as

$$\left. \begin{aligned} \hat{\mathbf{c}}^{k,0} &= \mathbf{0}, \\ \hat{\mathbf{c}}^{k,s} &= \mathcal{C}^s(\mathbf{z}^k, \hat{\mathbf{c}}^{k,s-1}), \quad s \in [R], \\ \mathbf{z}^{k+1} &= \mathcal{A}(\mathbf{z}^k, \hat{\mathbf{c}}^{k,1}, \dots, \hat{\mathbf{c}}^{k,R}). \end{aligned} \right\} \begin{array}{l} \text{(multiple communication rounds)} \\ \text{(computation step)} \end{array}$$

Absorbing the communication signals $\hat{\mathbf{c}}^{k,s}$ in the mapping \mathcal{A} , we can finally write the above system as a fixed-point iterate on the \mathbf{z} -variables only:

$$\mathbf{z}^{k+1} = \tilde{\mathcal{A}}(\mathbf{z}^k) \triangleq \mathcal{A}(\mathbf{z}^k, \mathcal{C}^1(\mathbf{z}^k, \mathbf{0}), \dots, \mathcal{C}^R(\mathbf{z}^k, \mathcal{C}^{R-1}(\mathbf{z}^k, \dots \mathcal{C}^1(\mathbf{z}^k, \mathbf{0}) \dots))). \quad (\text{M}')$$

Under suitable conditions, the iterates (M') convergence to fixed-points $\mathbf{z}^\infty = \tilde{\mathcal{A}}(\mathbf{z}^\infty)$ of the mapping $\tilde{\mathcal{A}}$, possibly constrained to a set $\mathcal{Z} \ni \mathbf{z}^\infty$. The convergence rate depends on the properties of $\tilde{\mathcal{A}}$; here we focus on *linear* convergence, which can be established under the following standard condition.

Assumption 1. *Let $\tilde{\mathcal{A}} : \mathcal{Z} \rightarrow \mathcal{Z}$; the following hold: (i) $\tilde{\mathcal{A}}$ admits a fixed-point \mathbf{z}^∞ ; and (ii) $\tilde{\mathcal{A}}$ is λ -pseudo-contractive on \mathcal{Z} w.r.t. some norm $\|\bullet\|$, that is, there exists $\lambda \in (0, 1)$ such that*

$$\|\tilde{\mathcal{A}}(\mathbf{z}) - \mathbf{z}^\infty\| \leq \lambda \cdot \|\mathbf{z} - \mathbf{z}^\infty\|, \quad \forall \mathbf{z} \in \mathcal{Z}.$$

*Without loss of generality, the norm $\|\bullet\|$ is scaled such that $\|\bullet\|_2 \leq \|\bullet\|$.*³

The following convergence result follows readily from Assumption 1 and [53, Ch. 3, Prop. 1.2].

Theorem 2. *Let $\tilde{\mathcal{A}} : \mathcal{Z} \rightarrow \mathcal{Z}$ satisfy Assumption 1. Then: i) the fixed point \mathbf{z}^∞ is unique; and ii) the sequence $\{\mathbf{z}^k\}$ generated by the update (M') converges Q -linearly to \mathbf{z}^∞ w.r.t. the norm $\|\bullet\|$ at rate λ , i.e., $\|\mathbf{z}^{k+1} - \mathbf{z}^\infty\| \leq \lambda \cdot \|\mathbf{z}^k - \mathbf{z}^\infty\|$.*

Discussion: The algorithmic framework (M) encompasses a variety of distributed algorithms, while Theorem 2 captures their convergence properties; in addition to the schemes covered by (M0), (M) can also represent EXTRA [43] and its proximal version [47], NEXT [15]–[17], DIGing [45], NIDS [49], and primal-dual schemes such as [42]. Appendix D provides specific expressions for the mappings \mathcal{A} and \mathcal{C}^s for each of the above algorithms, along with their convergence properties under Theorem 2; here, we elaborate on the NEXT algorithm (3) as an

³This is always possible since $\|\bullet\|$ is a norm defined on a finite-dimensional field.

example. It can be rewritten in the form (M) by using $R = 2$ rounds of communications and letting

$$\mathbf{z}_i^k = \begin{bmatrix} \mathbf{x}_i^k \\ \mathbf{y}_i^k \end{bmatrix}, \quad \hat{\mathbf{c}}_i^{k,1} = \mathbf{x}_i^k - \gamma \mathbf{y}_i^k, \quad \hat{\mathbf{c}}_i^{k,2} = \mathbf{y}_i^k + \nabla f_i \left(\sum_{j \in \mathcal{N}_i} w_{ij} \hat{\mathbf{c}}_j^{k,1} \right) - \nabla f_i(\mathbf{x}_i^k), \text{ and}$$

$$\mathcal{A}_i(\mathbf{z}_i^k, \hat{\mathbf{c}}_{\mathcal{N}_i}^{k,1}, \hat{\mathbf{c}}_{\mathcal{N}_i}^{k,2}) = \begin{bmatrix} \sum_{j \in \mathcal{N}_i} w_{ij} \hat{\mathbf{c}}_j^{k,1} \\ \sum_{j \in \mathcal{N}_i} w_{ij} \hat{\mathbf{c}}_j^{k,2} \end{bmatrix}.$$

III. A GENERAL DISTRIBUTED ALGORITHMIC FRAMEWORK: QUANTIZED COMMUNICATIONS

In this section, we equip the distributed algorithmic framework (M) with quantized communications. The communication channel between any two agents is modeled as a noiseless digital channel; only quantized signals are received with no errors. This means that, in each of the communication rounds, the signals $\hat{\mathbf{c}}_j^{k,1}, \dots, \hat{\mathbf{c}}_j^{k,R}$, $j \in \mathcal{N}_i$, received by agent i no longer coincide with the intended, unquantized ones $\mathcal{C}_j^1(\mathbf{z}_j^k, \mathbf{0}_{\mathcal{N}_j}), \dots, \mathcal{C}_j^R(\mathbf{z}_j^k, \hat{\mathbf{c}}_{\mathcal{N}_j}^{k,R-1})$, generated at the transmitter side of agents $j \in \mathcal{N}_i$. This calls for a proper encoding/decoding mechanism that transfers, via quantized communications, the aforementioned unquantized signals at the receiver sides with limited distortion. Here, we leverage differential encoding/decoding techniques [22] coupled with a novel finite-level quantization mechanism.

We begin recalling the idea of quantized differential encoding/decoding in the context of a point-to-point communication—the same mechanism will be then embedded in the communication of the distributed multi-agent framework (M). Consider a transmitter-receiver pair; let \mathbf{c}^k be the unquantized information generated at iteration k , intended to be transferred to the receiver over the digital channel, and let $\hat{\mathbf{c}}^k$ be the estimate of \mathbf{c}^k , built using quantized information. The differential encoding/decoding rule reads: $\hat{\mathbf{c}}^0 = \mathbf{0}$, and for $k = 1, \dots$,

$$\begin{cases} \mathbf{q}^k &= \mathcal{Q}^k(\mathbf{c}^k - \hat{\mathbf{c}}^{k-1}), \\ \hat{\mathbf{c}}^k &= \hat{\mathbf{c}}^{k-1} + \mathbf{q}^k, \end{cases} \quad (4)$$

where \mathcal{Q}^k is the quantization operator (a map from real numbers to the set of quantized points), possibly dependent on iteration k . In words, the encoder quantizes at each iteration the “prediction” error $\mathbf{c}^k - \hat{\mathbf{c}}^{k-1}$ rather than the current estimate \mathbf{c}^k , generating the quantized signal \mathbf{q}^k , which is then transmitted over the digital channel. The estimate $\hat{\mathbf{c}}^k$ of \mathbf{c}^k is built from \mathbf{q}^k using a one-step prediction rule. The rationale of this decoding rule is that, for negligible quantization

Algorithm 1 Distributed Algorithmic Framework with Quantized Communications

Initialization: $\hat{\mathbf{c}}^{-1,s} \triangleq \mathbf{0}$, for all $s \in [R]$; and $\mathbf{z}^0 \in \mathcal{Z}$. Set $k = 0$;

Iteration $k \rightarrow k + 1$

(S.1): Multiple communication rounds

for $s = 1, \dots, R$, each agent i :

- Computes $\mathbf{c}_i^{k,s} = \mathcal{C}_i^s(\mathbf{z}_i^k, \hat{\mathbf{c}}_{\mathcal{N}_i}^{k,s-1})$ [with $\hat{\mathbf{c}}_i^{k,0} \triangleq \mathbf{0}$];
- Generates $\mathbf{q}_i^{k,s} = \mathcal{Q}_i^k(\mathbf{c}_i^{k,s} - \hat{\mathbf{c}}_i^{k-1,s})$ and broadcasts it to its neighbors $j \in \mathcal{N}_i$;
- Upon receiving the signals $\mathbf{q}_j^{k,s}$ from its neighbors $j \in \mathcal{N}_i$, it reconstructs $\hat{\mathbf{c}}_j^{k,s}$ as

$$\hat{\mathbf{c}}_j^{k,s} = \hat{\mathbf{c}}_j^{k-1,s} + \mathbf{q}_j^{k,s}, \quad j \in \mathcal{N}_i;$$

end

(S.2): Computation Step

Each agent i updates its own \mathbf{z}_i^{k+1} according to

$$\mathbf{z}_i^{k+1} = \mathcal{A}_i(\mathbf{z}_i^k, \hat{\mathbf{c}}_{\mathcal{N}_i}^{k,1}, \dots, \hat{\mathbf{c}}_{\mathcal{N}_i}^{k,R}).$$

errors $\mathbf{q}^k = \mathcal{Q}^k(\mathbf{c}^k - \hat{\mathbf{c}}^{k-1}) \approx \mathbf{c}^k - \hat{\mathbf{c}}^{k-1}$, the estimate reads $\hat{\mathbf{c}}^k = \hat{\mathbf{c}}^{k-1} + \mathbf{q}^k \approx \hat{\mathbf{c}}^{k-1} + \mathbf{c}^k - \hat{\mathbf{c}}^{k-1} = \mathbf{c}^k$. Note that, since \mathbf{q}^k is received unaltered, $\hat{\mathbf{c}}^k$ is identical at the transmitter's and receiver's sides.

We can now introduce our distributed algorithmic framework using quantized communications, as described in Algorithm 1; it embeds the differential encoding/decoding rule (4) in each communication round of model (M). The fixed-point based formulation of Algorithm 1 then reads: for $i \in [m]$,

$$\left. \begin{aligned} \mathbf{c}_i^{k,1} &= \mathcal{C}_i^1(\mathbf{z}_i^k, \mathbf{0}_{\mathcal{N}_i}), \\ \hat{\mathbf{c}}_i^{k,1} &= \hat{\mathbf{c}}_i^{k-1,1} + \mathcal{Q}_i^k(\mathbf{c}_i^{k,1} - \hat{\mathbf{c}}_i^{k-1,1}), \\ &\vdots \\ \mathbf{c}_i^{k,R} &= \mathcal{C}_i^R(\mathbf{z}_i^k, \hat{\mathbf{c}}_{\mathcal{N}_i}^{k,R-1}), \\ \hat{\mathbf{c}}_i^{k,R} &= \hat{\mathbf{c}}_i^{k-1,R} + \mathcal{Q}_i^k(\mathbf{c}_i^{k,R} - \hat{\mathbf{c}}_i^{k-1,R}), \end{aligned} \right\} \text{(multiple communication rounds)} \quad (5)$$

$$\mathbf{z}_i^{k+1} = \mathcal{A}_i(\mathbf{z}_i^k, \hat{\mathbf{c}}_{\mathcal{N}_i}^{k,1}, \dots, \hat{\mathbf{c}}_{\mathcal{N}_i}^{k,R}), \quad \text{(computation step).}$$

Stacking agents' state-variables \mathbf{z}_i , signals \mathbf{c}_i and $\hat{\mathbf{c}}_i$, and mappings \mathcal{C}_i^s , \mathcal{A}_i , and \mathcal{Q}_i^k into the

respective vectors \mathbf{z} , \mathbf{c} , $\hat{\mathbf{c}}$, \mathcal{C}^s , \mathcal{A} , and \mathcal{Q}^k , we can rewrite (5) in compact form as

$$\left. \begin{aligned} \hat{\mathbf{c}}^{k,0} &= \mathbf{0}, \\ \mathbf{c}^{k,s} &= \mathcal{C}^s(\mathbf{z}^k, \hat{\mathbf{c}}^{k,s-1}), \\ \hat{\mathbf{c}}^{k,s} &= \hat{\mathbf{c}}^{k-1,s} + \mathcal{Q}^k(\mathbf{c}^{k,s} - \hat{\mathbf{c}}^{k-1,s}), \quad s \in [R], \\ \mathbf{z}^{k+1} &= \mathcal{A}(\mathbf{z}^k, \hat{\mathbf{c}}^{k,1}, \dots, \hat{\mathbf{c}}^{k,R}). \end{aligned} \right\} \begin{array}{l} \text{(multiple communication rounds)} \\ \text{(computation step).} \end{array} \quad (\text{Q-M})$$

Model (Q-M) paves the way to a unified design and convergence analysis of several distributed algorithms—all the schemes cast in the form (M)—employing quantization in the communications, as elaborated next.

A. Convergence Analysis

We begin by establishing sufficient conditions on the quantized mapping \mathcal{Q}^k and algorithmic functions \mathcal{A} and \mathcal{C} in (Q-M) to preserve linear convergence

- **On the quantization mapping \mathcal{Q}^k .** A first critical choice is the quantizer \mathcal{Q} (we omit the dependence on k for notation simplicity), including both random and deterministic quantization rules (the latter as special cases of the former). For random quantization, the function $\mathcal{Q}_i(\mathbf{x})$, $i \in [m]$, is a random variable for any given $\mathbf{x} \in \mathbb{R}^d$, defined on a suitable probability space (generally dependent on \mathbf{x}). We propose the following novel *biased compression rule* (BC-rule), for each agent i .

Definition 3 (Biased compression rule). Given $\mathbf{x} \in \mathbb{R}^d$, $\mathcal{Q}(\mathbf{x})$ (possibly, a random variable defined on a suitable probability space) satisfies the BC-rule with bias $\eta \geq 0$ and compression rate $\omega \in [0, 1)$ if

$$\sqrt{\mathbb{E}[\|\mathcal{Q}(\mathbf{x}) - \mathbf{x}\|_2^2]} \leq \sqrt{d}\eta + \omega\|\mathbf{x}\|_2, \quad \forall \mathbf{x} \in \mathbb{R}^d. \quad (6)$$

When $\mathcal{Q}(\mathbf{x})$ is a deterministic map, (6) reduces to

$$\|\mathcal{Q}(\mathbf{x}) - \mathbf{x}\|_2 \leq \sqrt{d}\eta + \omega\|\mathbf{x}\|_2, \quad \forall \mathbf{x} \in \mathbb{R}^d. \quad (7)$$

Roughly speaking, the bias η determines the basic spacing between quantization points, uniform across the entire domain. On the other hand, the compression term ω adds a nonuniform spacing between quantization points: quantization points farther away from $\mathbf{0}$ will have more separation.

The BC-rule encompasses and generalizes several existing compression and quantization rules proposed in the literature for specific algorithms, deterministic [10], [12]–[14], [18], [20], [22],

[24], [25], [27], [28], [33]–[36], [38], [40] and random [6]–[10], [19], [21], [23], [26], [29]–[32], [35]–[37], [39]–[41] ones. Specifically, **(i)** the compression rules proposed in [6]–[10], [32], [35]–[37], [39]–[41] (resp. [10], [33]–[36], [38], [40]) can be interpreted as *unbiased* instances of (6) [resp. (7)], i.e., corresponding to $\eta = 0$. The proof of Lemma 7 in Sec. IV will show that such special instances can only be implemented using *infinite* quantization points (hence number of bits). **(ii)** On the other hand, the quantization rules in [19], [21], [23], [26], [29]–[31] (resp. [12]–[14], [18], [20], [22], [24], [25], [27], [28]) are special cases of the BC-rule (6) [resp. (7)], with $\omega = 0$. While they can be implemented using a finite number of bits, they do not take advantage of the degree of freedom offered by the compression rate ω , a fact that will be numerically shown to lead to more communication-efficient schemes.

• **On the algorithmic mappings \mathcal{A} and \mathcal{C}^s .** Our analysis will require some standard conditions on the mappings \mathcal{A} and \mathcal{C}^s (in addition to Assumption 1) to preserve linear convergence under quantization. Roughly speaking, the functions \mathcal{A} and \mathcal{C}^s should vary smoothly with respect to perturbations in their arguments, so that small quantization errors result in small deviations from the trajectory of the unquantized algorithm. Specifically, we postulate the following.⁴

Assumption 4. *There exists a constant $L_A \geq 0$ such that, for every $s \in [R]$, it holds*

$$\|\mathcal{A}(\mathbf{z}, \mathbf{c}^1, \dots, \mathbf{c}^{s-1}, \mathbf{c}^s, \mathbf{c}^{s+1}, \dots, \mathbf{c}^R) - \mathcal{A}(\mathbf{z}, \mathbf{c}^1, \dots, \mathbf{c}^{s-1}, \mathbf{c}^{s'}, \mathbf{c}^{s+1}, \dots, \mathbf{c}^R)\| \leq L_A \|\mathbf{c}^s - \mathbf{c}^{s'}\|_2, \quad (8)$$

for all $\mathbf{c}^s, \mathbf{c}^{s'} \in \mathbb{R}^{md}$, uniformly with respect to $\mathbf{z} \in \mathcal{Z}$, and $\mathbf{c}^1, \dots, \mathbf{c}^{s-1}, \mathbf{c}^{s+1}, \dots, \mathbf{c}^R \in \mathbb{R}^{md}$.

Assumption 5. *There exist constants $L_C, L_Z \geq 0$ such that*

$$\|\mathcal{C}^s(\mathbf{z}, \mathbf{c}) - \mathcal{C}^s(\mathbf{z}, \mathbf{c}')\|_2 \leq L_C \|\mathbf{c} - \mathbf{c}'\|_2, \quad \forall \mathbf{c}, \mathbf{c}' \in \mathbb{R}^{md}, \quad (9)$$

$$\|\mathcal{C}^s(\mathbf{z}, \mathbf{c}) - \mathcal{C}^s(\mathbf{z}', \mathbf{c})\|_2 \leq L_Z \|\mathbf{z} - \mathbf{z}'\|_2, \quad \forall \mathbf{z}, \mathbf{z}' \in \mathcal{Z}, \quad (10)$$

uniformly with respect to $\mathbf{z} \in \mathcal{Z}$ and $\mathbf{c} \in \mathbb{R}^{md}$, respectively.

These assumptions are quite mild, and satisfied by a variety of existing distributed algorithms, as we will show in Appendix D. We are now ready to introduce our main convergence result.

⁴For the sake of notation, the constants L_A, L_C and L_Z defined in Assumptions 4 and 5 are assumed to be independent of the index s (communication round). Our convergence results can be readily extended to constants dependent on s .

Theorem 6. Let $\{\mathbf{z}^k\}$ be the sequence generated by Algorithm 1 under Assumptions 1, 4, and 5, with \mathcal{Q}^k satisfying the BC-rule (6) with bias $\eta = \eta^0 \cdot (\sigma)^k$ and compression rate $\omega \in [0, \bar{\omega}(\sigma))$, for some $\sigma \in (\lambda, 1)$ and $\eta^0 > 0$, where $\bar{\omega}(\sigma)$ is defined as

$$\bar{\omega}(\sigma) \triangleq \frac{\sigma}{R} \cdot \frac{\sigma - \lambda}{\sigma - \lambda + 2L_A L_Z [R \max\{1, (2L_C)^{R-1}\}]^2}. \quad (11)$$

Then,

$$\sqrt{\mathbb{E}[\|\mathbf{z}^k - \mathbf{z}^\infty\|_2^2]} \leq V_0 \cdot (\sigma)^k, \quad k = 0, 1, \dots,$$

where V_0 is a positive constant, whose expression is given in (35), Appendix A.

Proof: See Appendix A. ■

Note that, when the deterministic instance of the BC-rule is used [see (7)], the convergence rate reads $\|\mathbf{z}^k - \mathbf{z}^\infty\|_2 \leq V_0 \cdot (\sigma)^k$, for all $k = 0, 1, \dots$.

Theorem 6 shows that linear convergence is achievable when quantized communications are performed in distributed optimization, provided that the bias η and compression rate ω of the BC-rule are chosen suitably. Specifically, the bias η should shrink linearly (at rate σ) and the compression rate ω should be sufficiently small, so that the quantization errors along the iterates will not accumulate disruptively. The final linear convergence rate is determined by σ , which is larger than rate λ achievable by the same scheme that does not use any quantization. As expected, there is a tension between the amount of quantization/compression of the transmitted signals (measured by η and ω) and the resulting linear convergence rate σ : the slower the decay of η (resulting in less stringent quantization requirements), the slower the convergence rate of the algorithm (the larger σ). However, as we will see in Theorem 12, the price to pay to achieve faster convergence is communication cost.

Theorem 6 certifies linear convergence in terms of number of iterations; building on this result, in the forthcoming sections we study the communication complexity of the schemes (Q-M)—the total number of bits needed to reach an ε -solution of problem (P). This depends on the specific quantizer used in the algorithms. The next section introduces a novel quantizer that satisfies the BC-rule whi using the minimum number of quantization points, and a communication-efficient bit-encoding/decoding scheme. When embedded in (Q-M), the proposed quantization leads to linearly convergent distributed algorithms whose communication complexity compares favorably with that of existing ad-hoc schemes (Sec. V).

IV. NON-UNIFORM QUANTIZER WITH ADAPTIVE ENCODING/DECODING

As discussed in Sec. III, the BC-rule encompasses a variety of quantizer designs. In this section, we propose a scalar quantizer that fulfills the BC-rule with minimum number of quantization points (Sec. IV-A). The quantizer is then coupled with a communication-efficient bit-encoding/decoding rule which enables transmission on the digital channel (Sec. IV-B). We refer to the proposed quantizer coupled with the encoding/decoding scheme as *Adaptive encoding Non-uniform Quantization* (ANQ).

A. Quantizer design

Since no information is assumed on the distribution of the input signal, a natural approach is to quantize each vector signal component-wise. We design such a scalar quantizer $\mathcal{Q} : [-\delta, \delta] \rightarrow \mathbb{Q}$ under the BC-rule by minimizing the number of quantization points $|\mathbb{Q}|$ for a fixed input dynamic δ . Equivalently, we seek \mathcal{Q} that maximizes δ , for a given number $N = |\mathbb{Q}|$ of quantization points while satisfying the BC-rule. The optimal scalar deterministic and probabilistic quantizer designs satisfying the BC-rule are provided in Lemma 7 and Lemma 8, respectively. For convenience, we focus on the case of N odd; the case of N even is provided in Appendices B-A and B-B.

Lemma 7 (Deterministic Quantizer). *Let $\mathcal{Q} : [-\delta, \delta] \rightarrow \mathbb{Q}$. The maximum range δ that can be quantized using $|\mathbb{Q}| = N$ points while fulfilling the BC-rule (7) with bias $\eta \geq 0$ and compression rate $\omega \in [0, 1)$ is*

$$\delta(\eta, \omega, N) = \frac{q_{(N-1)/2} + q_{(N+1)/2}}{2}, \quad (12)$$

with quantization points

$$q_\ell = -q_{-\ell} = \frac{\eta}{\omega} \left[\left(\frac{1+\omega}{1-\omega} \right)^\ell - 1 \right], \quad \ell \geq 0. \quad (13)$$

The resulting optimal quantization rule reads: $x \mapsto \mathcal{Q}(x) = q_{\ell(x)}$, with

$$\ell(x) = \text{sign}(x) \cdot \left\lceil \frac{\ln(1-\omega) + \ln(1 + \frac{\omega}{\eta}|x|)}{\ln(1+\omega) - \ln(1-\omega)} \right\rceil. \quad (14)$$

Proof: See Appendix B-A. ■

From Lemma 7, one infers that the optimal quantizer has quantization points non-uniformly spaced—hence the name ANQ—and maps inputs x to the nearest q_ℓ .

We next study the optimal probabilistic quantizer design under the BC-rule (6).

Lemma 8 (Probabilistic Quantizer). *For any given $x \in [-\delta, \delta]$, let $\mathcal{Q}(x) \in \mathbb{Q}$ be a random variable defined on a suitable probability space. The maximum range δ that can be quantized using $|\mathbb{Q}| = N$ points while fulfilling the BC-rule (6) with $\mathbb{E}[\mathcal{Q}(x)] = x$ with bias $\eta \geq 0$ and compression rate $\omega \in [0, 1)$ is*

$$\delta(\eta, \omega, N) = q_{(N-1)/2}, \quad (15)$$

with quantization points

$$q_\ell = -q_{-\ell} = \frac{\eta}{\omega} \left[\left(\sqrt{1 + (\omega)^2} + \omega \right)^{2\ell} - 1 \right], \quad \ell \geq 0. \quad (16)$$

The resulting optimal quantization rule reads: $x \mapsto \mathcal{Q}(x) = q_{\ell(x)}$, with

$$\ell(x) = \begin{cases} \ell - 1, & \text{w.p. } \frac{q_\ell - x}{q_\ell - q_{\ell-1}}; \\ \ell, & \text{w.p. } \frac{x - q_{\ell-1}}{q_\ell - q_{\ell-1}}, \end{cases} \quad \text{and} \quad \ell = \text{sign}(x) \left\lceil \frac{\ln(1 + \frac{\omega}{\eta}|x|)}{2 \ln(\sqrt{1 + (\omega)^2} + \omega)} \right\rceil. \quad (17)$$

Proof: See Appendix B-B. ■

The probabilistic quantizer above has quantization points non-uniformly spaced, and maps x to one of the two nearest quantization points, selected randomly such that $\mathbb{E}[\mathcal{Q}(x)] = x$.

Note that for the proposed deterministic and probabilistic quantizers, the index $\ell(x)$ is sufficient information to infer the quantization point $q_{\ell(x)}$. In Sec. IV-B we present a communication-efficient finite bit-encoding/decoding scheme to transmit $\ell(x)$ over the digital channel.

From Lemma 7 and Lemma 8, it is clear that the optimal quantizer uses a finite number of quantization points (and thus of bits) when $\eta > 0$. This contrasts with the compression rule (2), which cannot be implemented using a *finite* number of quantization points (in fact, in this case $\delta(0, \omega, N) = 0$ for any finite N). The next corollary formalizes this negative result.

Corollary 9 (Converse). *No quantizer using a finite number of quantization points can satisfy the compression rule (2). Therefore, the compression rules in [6]–[10], [32]–[38], [41] cannot be implemented using a finite number of bits.*

Proof. See Appendix B-C. □

B. Adaptive encoding scheme

It remains to design an encoding/decoding scheme mapping the index $\ell(x)$ into a finite-bit representation, to be transmitted over the digital channel. To do so, we adopt an adaptive number of bits, based upon the value of $\ell(x)$, as detailed next.

We assume that a constellation $\mathbb{S} = [S] \cup \{0\}$ of $S + 1$ symbols is used, with $S \geq 2$ (this might be obtained as $\mathbb{S} \equiv (\tilde{\mathbb{S}})^w$, by concatenating sequences of w symbols from a smaller constellation $\tilde{\mathbb{S}}$). We use the symbol 0 to indicate the end of an information sequence, and the remaining S symbols $[S]$ to encode the value of $\ell(x)$. Defining $\tilde{\mathcal{L}}_{-1} \equiv \emptyset$, let

$$\tilde{\mathcal{L}}_b \equiv \left\{ - \left\lceil \frac{S^{b+1} - 1}{2(S - 1)} \right\rceil + 1, \dots, \left\lfloor \frac{S^{b+1} - 1}{2(S - 1)} \right\rfloor \right\}, \quad b = 0, 1, \dots,$$

and

$$\mathcal{L}_b = \tilde{\mathcal{L}}_b \setminus \tilde{\mathcal{L}}_{b-1}, \quad b = 0, 1, \dots \quad (18)$$

It is not difficult to check that $\{\mathcal{L}_b : b = 0, 1, \dots\}$ creates a partition of \mathbb{Z} and $|\mathcal{L}_b| = (S)^b$. Therefore, a natural way to encode $\ell(x)$ is to use a unique sequence of b symbols from $[S]$, i.e., $[s_1, \dots, s_b] \in [S]^b$, where b is the unique integer such that $\ell(x) \in \mathcal{L}_b$. The transmitted sequence coding $\ell(x)$ reads then $[s_1, \dots, s_b, 0]$, where 0 marks the end of the information sequence.

Upon receiving this sequence, the receiver can detect the start and end of the information symbols, and decode the associated $\ell(x)$ by inverting the symbol-mapping. The communication cost to transmit the index $\ell(x) \in \mathcal{L}_b$ is thus $b + 1$ (symbols), which leads to the following upper bound on the overall communication cost incurred by each agent i to quantize and encode a d -dimensional vector \mathbf{x} . Again, we focus on the case when N is odd; the other case is provided in the proof in Appendix C-D.

Lemma 10. *The number of bits $C(\mathbf{x})$ required by the ANQ with bias $\eta \geq 0$ and compression rate $\omega \geq 0$ and constellation of $S + 1$ symbols to quantize and encode an input signal $\mathbf{x} \in \mathbb{R}^d$ is upper bounded by*

(i) Deterministic quantizer:

$$C(\mathbf{x}) \leq \log_2(S + 1) \left[3d + d \log_S \left(2 + \frac{\ln(1 - \omega) + \ln \left(1 + \frac{\omega \|\mathbf{x}\|_2}{\sqrt{d}\eta} \right)}{\ln(1 + \omega) - \ln(1 - \omega)} \right) \right] \quad \text{bits}; \quad (19)$$

(ii) Probabilistic quantizer with $\mathbb{E}[\mathcal{Q}(\mathbf{x})] = \mathbf{x}$:

$$C(\mathbf{x}) \leq \log_2(S + 1) \left[3d + d \log_S \left(2 + \frac{\ln \left(1 + \frac{\omega \|\mathbf{x}\|_2}{\sqrt{d}\eta} \right)}{2 \ln \left(\sqrt{1 + (\omega)^2} + \omega \right)} \right) \right] \quad \text{bits}, \quad a.s.. \quad (20)$$

Proof. See Appendix C-D. □

Compared with existing deterministic quantizers [12], [13] that are special cases of the BC-rule (with $\omega = 0$), the proposed ANQ adapts the number of bits to the input signal-less bits

for smaller input signals (mapped to smaller ℓ) and more bits for larger ones (mapped to larger ℓ)—rather than using a fixed number of bits determined by the worst-case input signal [12], [13]. This leads to more communication-efficient schemes, as certified by Theorem 13.

Comparing the communication cost for the probabilistic and deterministic quantizers, it can be shown that the former incurs in a larger cost than the latter. This is due to the fact that in the probabilistic ANQ, the need to enforce the constraint $\mathbb{E}[\mathcal{Q}(x)] = x$ makes the solution less optimal than the one for deterministic ANQ.

V. COMMUNICATION COMPLEXITY OF (Q-M) USING THE ANQ RULE

We now study communication complexity of the distributed schemes falling within the framework (Q-M) and using the ANQ to quantize communications. Our results complement Theorem 6 and are of two types: (i) first, we determine the number of bits/agent to be used by the ANQ at each iteration to guarantee linear convergence rate (in terms of iterations) of any algorithm within (Q-M) (Theorem 12); (ii) then, we provide the communication complexity in the setting of (i), that is, the total number of bits/agent transmitted to achieve an ε -solution of (P) (Theorem 13). Finally, we customize (ii) to some specific distributed algorithms within (Q-M) (Sec. V-A).

Throughout this section, all the results stated in terms of \mathcal{O} -notation are meant asymptotically when $m, d \rightarrow \infty$. Also, the following additional mild assumption is postulated, which is satisfied by a variety of existing algorithms, see Appendix D.

Assumption 11. *The constants L_A, L_C, L_Z and the initial conditions $\|\mathcal{C}^s(\mathbf{z}^0, \mathbf{0})\|_2$ and $\|\mathbf{z}^0 - \mathbf{z}^\infty\|$ satisfy*

$$L_A L_Z = \mathcal{O}(1), \quad L_C = \mathcal{O}(1), \quad \|\mathcal{C}^s(\mathbf{z}^0, \mathbf{0})\|_2 = \mathcal{O}(L_Z \sqrt{md}), \quad \forall s \in [R],$$

and $\|\mathbf{z}^0 - \mathbf{z}^\infty\| = \mathcal{O}(\sqrt{md})$.

Our first result on the number of bits transmitted at each iteration to sustain linear convergence is summarized next.

Theorem 12. *Instate the setting of Theorem 6, under the additional Assumption 11. Furthermore, suppose that the deterministic ANQ (or probabilistic ANQ with $\mathbb{E}[\mathcal{Q}(\mathbf{x})] = \mathbf{x}$) is used to quantize all the communications in (Q-M), with $\eta^0 = \Theta(L_Z(\sigma - \lambda))$ and ω such that $1 - \omega/\bar{\omega}(\sigma) = \Omega(1)$.*

Then, linear convergence $\sqrt{\mathbb{E}[\|\mathbf{z}^k - \mathbf{z}^\infty\|_2^2]} = \mathcal{O}(\sqrt{md} \cdot (\sigma)^k)$, $k = 0, 1, \dots$, is achieved with an average number of bits/agent at every iteration k given by

$$\mathcal{O}\left(d \log_2\left(1 + \frac{1}{\sigma(\sigma - \lambda)}\right)\right). \quad (21)$$

Proof: See Appendix C-A. ■

The following comments are in order.

(i) As expected, the faster the quantized algorithm (smaller σ), the larger the communication cost incurred per iteration; in particular, when $\sigma \rightarrow \lambda$, the number of bits required to sustain linear convergence at rate σ grows indefinitely. In other words, an infinite number of bits is required if a quantized distributed scheme (Q-M) wants to match the convergence rate of its unquantized counterpart.

(ii) It is interesting to contrast the communication efficiency (bits transmitted per iteration) of the proposed model (Q-M) equipped with the ANQ with that of existing schemes. Specifically, the schemes in [12], [13] use $\mathcal{O}(d \log_2(1 + \frac{\sqrt{md}}{\sigma(\sigma - \lambda)}))$ bits/agent/iteration over mesh networks while $\mathcal{O}(d \log_2(1 + \frac{\sqrt{d}}{\sigma(\sigma - \lambda)}))$ bits/agent/iteration are required in the analysis of [12] over star networks. Both are less favorable than (21). This can be attributed to the fact that the ANQ adapts the number of bits to the input signal rather than adopting a constant number of bits for any input signal as [12], [13].

(iii) Theorem 12 reveals a tension between convergence rate (the closer σ to λ , the faster the algorithm) and number of transmitted bits per iteration (the larger σ , the smaller the cost). We provide a favorable choice of σ to exploit this trade-off and determine consequently the total number of transmitted bits/agent to achieve a target ε -accuracy.

Theorem 13. *Instate the setting of Theorem 12, with $R = \mathcal{O}(1)$ and σ chosen so that $\frac{(1-\lambda)^2}{(1-\sigma)(\sigma-\lambda)} = \mathcal{O}(1)$. Then, the following average number of (transmitted) bits/agent is sufficient for $\{\mathbf{z}^k\}$ to achieve $(1/m)\mathbb{E}[\|\mathbf{z}^k - \mathbf{z}^\infty\|_2^2] \leq \varepsilon$:*

$$\mathcal{O}\left(d \log_2\left(1 + \frac{1}{1-\lambda}\right) \frac{1}{1-\lambda} \log_2(d/\varepsilon)\right) \text{ bits/agent.} \quad (22)$$

Proof: See Appendix C-C. ■

The following comments are in order.

(i) Intuitively, Theorem 13 provides a range of values of σ to balance the conflicting effect on the convergence rate and communication cost per iteration resulting from too small or too large values of σ . The condition of the theorem can be satisfied, e.g., by choosing $\sigma = (1 + \lambda)/2$.

(ii) The term $d \cdot \log_2(1 + 1/(1 - \lambda))$ in (22) represents the number of bits/iteration, as postulated by Theorem 13, under the additional restriction on σ : the faster the unquantized algorithm (i.e., the smaller λ), the fewer bits are required. The second term $(1 - \lambda)^{-1} \log_2(d/\varepsilon)$ represents the total number of iterations required to achieve ε accuracy for the unquantized algorithm, with $\log_2(d)$ capturing the gap of the initial point from the fixed point; as expected, the number of iterations increases as the unquantized algorithm slows down (λ increases), the dimension d increases, and/or the target error ε decreases.

Nest, we customize Theorem 13 to some distributed algorithms within (Q-M).

A. Special cases of (Q-M) using the ANQ rule

1) GD over star-networks: Our first case study is the GD algorithm solving (P) (with $r = 0$) over star networks. The unquantized scheme reads

$$\mathbf{x}^{k+1} = \mathbf{x}^k - \frac{\gamma}{m} \sum_{i=1}^m \nabla f_i(\mathbf{x}^k), \quad (23)$$

with $\gamma \in (0, 2/L)$. In [12], it is shown that, when employed with the quantization scheme proposed therein, the resulting quantized GD achieves an ε -solution by transmitting on average

$$\mathcal{O}\left(\log_2\left(1 + \frac{d}{1 - \lambda}\right) \frac{d}{1 - \lambda} \log_2(d/\varepsilon)\right) \text{ bits/agent}. \quad (24)$$

The GD (23) is an instance of (M); therefore, we can employ quantization in the master-workers' communications and cast the resulting quantized algorithm in (Q-M). When the ANQ is used, a direct application of Theorem 13 leads to the following communication complexity.

Corollary 14 (GD over star networks). *The GD algorithm (23) employing quantization in the master-workers' communications using the ANQ with tuning as in Theorem 13 requires on average of*

$$\mathcal{O}\left(\log_2\left(1 + \frac{1}{1 - \lambda}\right) \frac{d}{1 - \lambda} \log_2(d/\varepsilon)\right) \text{ bits/agent}, \quad (25)$$

to reach an ε -solution of (P) (with $r = 0$).

A direct comparison of (24) and (25) shows that the proposed ANQ improves on the state-of-the-art deterministic quantizer with shrinking range developed in [12].

2) Distributed algorithms employing gradient correction: Our second example deals with distributed algorithms solving (P) (now possibly with $r \neq 0$) over mesh networks. We consider among the most popular ones, employing gradient correction in the optimization direction. Their

computational complexity when using the ANQ is summarized next—see Appendix D for a description of such algorithms.

Corollary 15 (mesh networks). *Consider any of the following algorithms using the ANQ in agents' communications, with parameters as specified in Theorem 13: the primal-dual algorithm (solving (P) with $r = 0$) [12]; the (Prox-)EXTRA, (Prox-)NEXT, (Prox-)DIGing, and (Prox-)NIDS [47] (for general (P) with $r \neq 0$). An ε -solution is achieved by transmitting on average*

$$\mathcal{O}\left(\log_2\left(1 + \frac{1}{1-\lambda}\right)\frac{d}{1-\lambda}\log_2(d/\varepsilon)\right) \text{ bits/agent.}$$

To our knowledge, Corollary 15 provides the first analytical result on the communication cost to achieve an ε -solution of Problem (P) by distributed algorithms over mesh networks. In particular, the schemes employing the proposed ANQ are the first algorithms using finite rate communications when applied to such a general class of optimization problems (with $r \neq 0$) and networks (mesh topology).

VI. NUMERICAL RESULTS

In this section, we validate numerically our theoretical findings and compare different distributed algorithms using quantization. We simulate two instances of (P): a least square and a logistic regression problem. The communication network is modelled by an undirected graph of $m = 20$ agents, generated by the Erdos-Renyi model with edge activating probability of 0.6. We measure performance of the algorithms using the following two metrics:

$$\text{MSE}^k \triangleq \frac{\sum_{i=1}^m \|\mathbf{x}_i^k - \mathbf{x}^*\|_2^2}{m\|\mathbf{x}^*\|_2^2} \quad \text{and} \quad C_{\text{cm}}(\varepsilon) \triangleq \sum_{k=0}^{k_\varepsilon} \sum_{s=1}^R \sum_{i=1}^m b_i^{k,s}, \quad (26)$$

where $k_\varepsilon \triangleq \min_{k \geq 0} \text{MSE}^k \leq \varepsilon$ and $b_i^{k,s}$ is the number of bits used by the quantizer for encoding the s th transmitted signal by agent i at iteration k .

A. Least square problem

Problem setting: Consider the following least square problem [instance of (P)] over networks:

$$f_i(\mathbf{x}) = \frac{1}{2}\|\mathbf{U}_i\mathbf{x} - \mathbf{v}_i\|_2^2 + \frac{0.01}{2}\|\mathbf{x}\|_2^2 \quad \text{and} \quad r(\mathbf{x}) = \alpha\|\mathbf{x}\|_1, \quad (27)$$

where $\mathbf{U}_i \in \mathbb{R}^{20 \times 40}$ and $\mathbf{v}_i \in \mathbb{R}^{1 \times 40}$ are the feature vector and observation measurements, respectively, accessible only by agent i . These are generated as follows [54]: $\mathbf{U}_1 \sim \mathcal{N}(\mathbf{0}, \frac{1}{\sqrt{1-\beta^2}}\mathbf{I})$ and, for $i > 1$, $\mathbf{U}_i|\mathbf{U}_{i-1} \sim \mathcal{N}(\beta\mathbf{U}_{i-1}, \mathbf{I})$, where $\beta = 0.3$. In this way, each row of $\mathbf{U} =$

$[\mathbf{U}_1, \dots, \mathbf{U}_{40}]$ is a Gaussian random vector with zero mean and covariance depending on β : larger β generates more ill-conditioned covariance matrices. Then, letting $\mathbf{x}_0 \in \mathbb{R}^{40}$ be the ground truth vector, generated as a sparse vector with 70% zero entries, and i.i.d. nonzero entries drawn from $\mathcal{N}(0, 1)$, we generate $\mathbf{v} = [\mathbf{v}_1, \dots, \mathbf{v}_{40}]$ as $\mathbf{v} | (\mathbf{U}, \mathbf{x}_0) \sim \mathcal{N}(\mathbf{U}\mathbf{x}_0, 0.04\mathbf{I})$. We let μ, L be the strong convexity and smoothness parameters of f_i , respectively.⁵

We test several distributed algorithms considering either smooth ($\alpha = 0$) or nonsmooth instances of the least square problem (27). In fact, most of the existing schemes are applicable only to smooth optimization problems. The free parameters of these algorithms are tuned as recommended in the original papers, unless otherwise stated; the weight matrix $\tilde{\mathbf{W}}$ used to mix the received signals is constructed according to the Metropolis-Hastings rule [55]; the number of bits transmitted by each scheme as reported below is per agent, per dimension, per iteration. For each quantized algorithm, we choose $\sigma = 0.99 \cdot \lambda + 0.01$, where $\lambda = (\text{MSE}^{100}/\text{MSE}^{50})^{0.01}$ is the numerical estimate of the convergence rate of its unquantized counterpart.

Smooth least square (Fig. 2a): We begin by considering the smooth least square problem and the following quantized schemes:

- 1) Q-Dual [12]: parameters are chosen as in [12, Theorem 1]—the averaged number of transmitted bits is 13.
- 2) ANQ-Dual: this is the primal-dual algorithm [42] equipped with the proposed deterministic ANQ (see Appendix D-F), with $\eta^0 = 0.01$ and $\omega = \bar{\omega}/2$ [recall that $\bar{\omega}$ is defined in (11)]—the average transmitted number of bits is 6.63.
- 3) Q-NEXT [13], with quantization as in [13, Theorem 4]—the average transmitted number of bits is 78.
- 4) ANQ-NEXT: this is the NEXT algorithm [15], [16], [46] quantized using the deterministic ANQ with $\eta^0 = 0.029$ and $\omega = \bar{\omega}/2$. The average transmitted number of bits is 15.69.
- 5) ANQ-NIDS: this is an instance of the NIDS algorithm [47], [49] equipped with the deterministic ANQ (see Appendix D-D) with parameters $\eta^0 = 0.001$ and $\omega = \bar{\omega}/2$. The transmitted average number of bits is 8.69.

As benchmark, we also simulated some of the unquantized instances of the algorithms listed above, namely:

⁵When f_i is μ_i -strongly convex and L_i -smooth, we let $\mu = \min_i \mu_i$ and $L = \max_i L_i$.

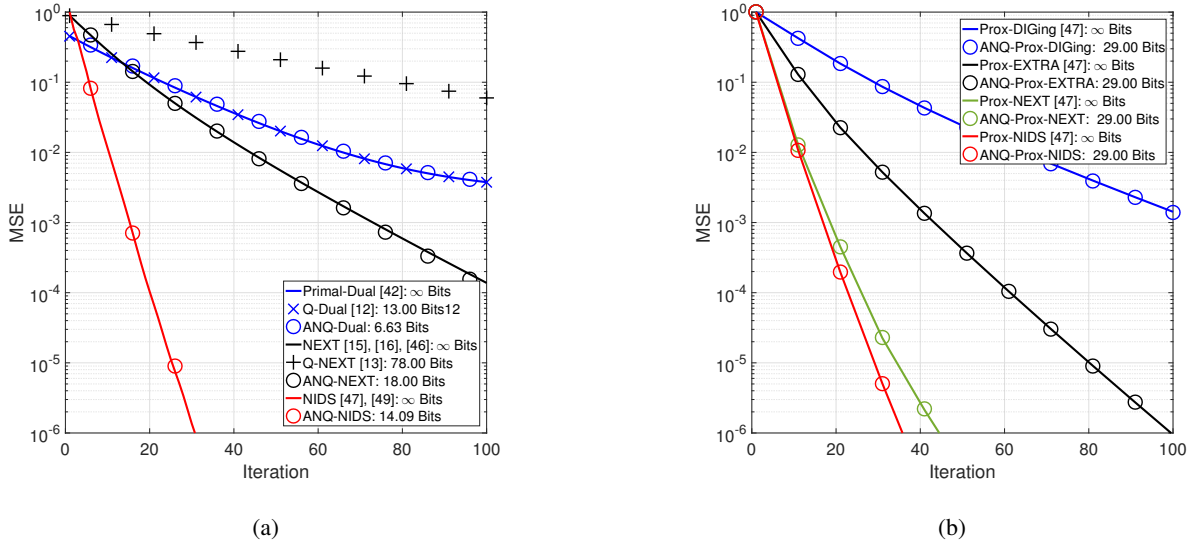


Fig. 2: Least square problem (27): MSE versus iterations for the smooth (a) and non-smooth (b) cases. Solid curves and markers refer to algorithms with exact and quantized communications, respectively.

- 6) Primal-Dual [42] with step-size $\gamma = 2L\mu/(\mu\rho_{m-1}(\mathbf{L}) + L\rho_1(\mathbf{L}))$ ([12, Proposition 2]), where \mathbf{L} is the graph Laplacian matrix associated with the graph.
- 7) NEXT [15], [16], [46] with step-size $\gamma = 0.0029$, manually tuned for fastest practical convergence.
- 8) NIDS [47], [49] with step-size $\gamma = \frac{2}{L+\mu}$ and mixing matrix $\mathbf{W} = [(1 + \nu)\mathbf{I} + (1 - \nu)\tilde{\mathbf{W}}]/2$, with $\nu = 0.001$.

In Fig. 2a, we plot the MSE versus iteration index k . Remarkably, all algorithms, when equipped with ANQ, incur in a negligible loss of convergence speed with respect to their unquantized counterpart. Comparing ANQ with the state-of-the-art quantized algorithms, we notice that ANQ is more communication-efficient than Q-NEXT and Q-Dual that instead use deterministic uniform quantizers with shrinking range: ANQ-NEXT (18 bits) and ANQ-Dual (6.63 bits) use fewer bits per iteration than Q-NEXT (13 bits) and Q-Dual (78 bits), respectively, despite converging faster.

Nonsmooth least square (Fig. 2b): We now move to the nonsmooth instance of (27), with $\alpha = 10^{-4}$. We tested the following quantized algorithms:

- 1) ANQ-Prox-EXTRA: this is an instance of the Prox-EXTRA algorithm [47] equipped with the deterministic ANQ (see Appendix D-A) with parameters $\eta^0 = 2.68 \times 10^{-5}$ and $\omega = \bar{\omega}/2$.
- 2) ANQ-Prox-NEXT: this is the Prox-NEXT algorithm [47] equipped with the deterministic

ANQ (see Appendix D-B) with parameters $\eta^0 = 2.85 \times 10^{-3}$ and $\omega = \bar{\omega}/2$.

- 3) ANQ-PROX-DIGing: this is the Prox-DIGing algorithm [47] equipped with the deterministic ANQ (see Appendix D-C) with parameters $\eta^0 = 3.65 \times 10^{-3}$ and $\omega = \bar{\omega}/2$.
- 4) ANQ-PROX-NIDS: this is the Prox-NIDS algorithm in [47] equipped with the deterministic ANQ (see Appendix D-D) with parameters $\eta^0 = 3.08 \times 10^{-5}$ and $\omega = \bar{\omega}/2$.

As benchmark, we also included the unquantized counterparts of the above algorithms; in all these schemes we used the weight matrix $\mathbf{W} = [(1 + \nu)\mathbf{I} + (1 - \nu)\tilde{\mathbf{W}}]/2$ with $\nu = 0.001$; the step-size is chosen according to [47], namely: $\gamma = \frac{2\rho_m(\mathbf{W})}{L + \mu\rho_m(\mathbf{W})}$ for Prox-EXTRA, $\gamma = \frac{2\rho_m(\mathbf{W}^2)}{L + \mu\rho_m(\mathbf{W}^2)}$ for Prox-DIGing, and $\gamma = \frac{2}{L + \mu}$ for Prox-NEXT and Prox-NIDS.

Fig. 2b plots the MSE achieved by all the algorithms versus the iteration index. As predicted, all four quantized schemes converge linearly. Remarkably, all of the ANQ-equipped algorithms incur in a negligible loss of convergence speed with respect to their unquantized counterparts, while transmitting only 29 bits per agent/dimension/iteration.

B. Logistic regression

We now consider the distributed logistic regression problem using the MNIST dataset [56]. This is an instance of (P) with

$$f_i(\mathbf{x}) = \frac{0.01}{2} \|\mathbf{x}\|_2^2 + \frac{1}{3000} \sum_{p=1}^{3000} \ln \left(1 + \exp \left(-v_{i,p} \mathbf{u}_{i,p}^\top \mathbf{x} \right) \right), \quad \text{and} \quad r(\mathbf{x}) = \alpha \|\mathbf{x}\|_1, \quad (28)$$

where $\mathbf{u}_{i,p} \in \mathbb{R}^{784 \times 1}$ and $v_{i,p} \in \{-1, 1\}$ are the feature vector and labels, respectively, only accessible by agent i . Here we implement the one-vs.-all scheme, i.e., the goal is to distinguish the data of label '0' from others. To generate $\mathbf{u}_{i,p}$, we first flatten each picture of size 28×28 in MNIST into a real feature vector of length $28 \times 28 = 784$, and then normalize it to unit l_2 norm. We then allocate equal number of feature vectors and labels to each agent.

Smooth logistic regression (Fig. 3a): We begin by considering the smooth logistic regression problem (28), with $\alpha = 0$. We tested the same algorithms (with the same tuning) as described in Sec. VI-A for the smooth least square problem. In Fig. 3a, we plot the MSE versus iteration index k . Consistently with the results in Fig. 2a, we notice the following facts. ANQ-NIDS achieves the fastest convergence, followed by ANQ-NEXT, ANQ-Dual, Q-Dual and Q-NEXT. Comparing our quantization method with existing ones on the same algorithm, we notice that the proposed ANQ is more communication-efficient than Q-NEXT and Q-Dual: ANQ-NEXT (14

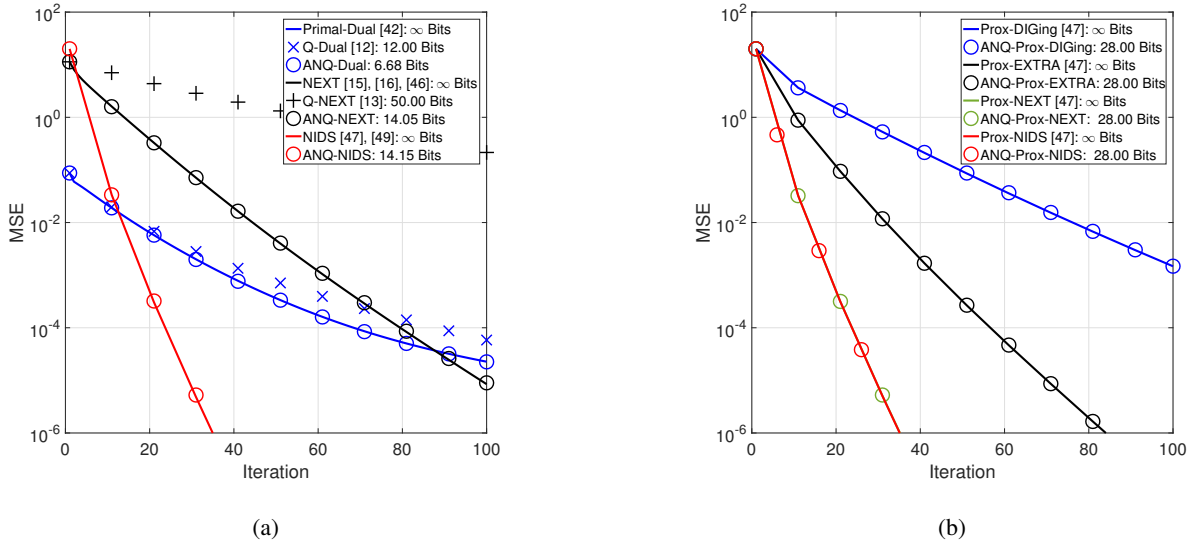


Fig. 3: Logistic regression (28): MSE versus iterations for the smooth (a) and non-smooth (b) cases. Solid curves and markers refer to algorithms with exact and quantized communications, respectively.

bits) and ANQ-Dual (6.7 bits) use fewer bits per iteration than Q-NEXT (50 bits) and Q-Dual (12 bits), despite converging faster.

Nonsmooth logistic regression (Fig. 3b): We now consider the nonsmooth instance of the logistic regression problem (28), with $\alpha = 10^{-4}$. We tested the same algorithms (with the same tuning) as described in Sec. VI-A for the nonsmooth least square problem. Fig. 3b plots the MSE achieved by all the algorithms versus iterations k . The results confirm the trends already commented in Fig. 2b.

C. Communication cost

We now study the effect of dimension d on the communication cost for different algorithms solving the nonsmooth least square problem (27), with $\alpha = 10^{-4}$. Note that the rate of an unquantized algorithm λ depends on both the weight matrix and the condition number $\kappa = L/\mu$, which depends itself on d . We chose the coefficient of the l_2 regularizer so as to make κ remain fixed across different d . The rest of the settings are the same as in Fig. 2b. Fig. 4 plots the communication cost versus d , for a target MSE-accuracy $\varepsilon = 10^{-8}$. One can observe that the communication cost for all algorithms scales roughly linearly with respect to the dimension, which is consistent with Theorem 13.

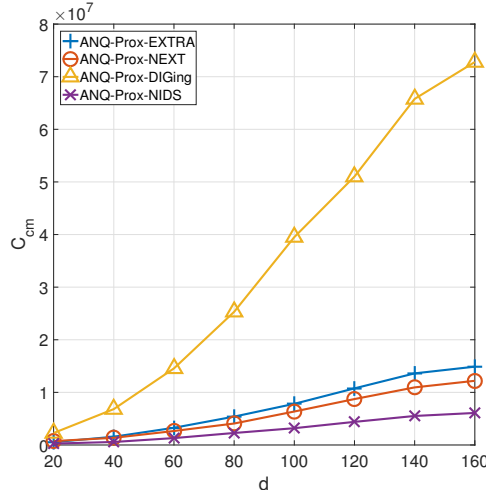


Fig. 4: Communication cost evaluation on nonsmooth least square problem with $\alpha = 10^{-4}$ versus d .

Finally, we investigate numerically the effect of σ and ω on the communication cost as defined in (26), for a target MSE-accuracy $\varepsilon = 10^{-8}$. We consider the ANQ-NIDS algorithm solving the least square problem (27), with $\alpha = 0$. Fig. 5a plots the communication cost versus σ with $\omega = \bar{\omega}/2$. Note that there is a sweet spot for σ , resulting in a saving of 64% with respect to the largest communication cost, which justifies the discussion in Sec. V that σ should be chosen away from λ and 1 in order to save on communication cost. Fig. 5a plots the communication cost (26) versus ω with $\sigma = 0.99 \times \lambda + 0.01$. It can be seen that, by optimizing the compression rate ω , a saving of 30% in communication cost can be obtained over a quantization scheme that employs no compression ($\omega = 0$). This observation numerically supports our BC-rule, which is more general than the deterministic/probabilistic quantizers that have no compression term.

VII. CONCLUSIONS

This paper proposes a black-box model and unified convergence analysis for a general class of linearly convergent algorithms subject to quantized communications. This generalizes existing algorithmic frameworks, which cannot deal with composite optimization problems and model distributed algorithms using historical information (e.g., EXTRA [43] and NEXT [15]). Quantization is addressed by proposing a novel *biased compression (BC)-rule* that preserves linear convergence of distributed algorithms while using a *finite* number of bits in each communication. In fact, we proved that most of existing quantization rules can be implemented only using an infinite number of bits. As special instance of the BC-rule, we also proposed a new (random) quantizer, the ANQ, coupled with a communication-efficient encoding scheme. The communication cost of

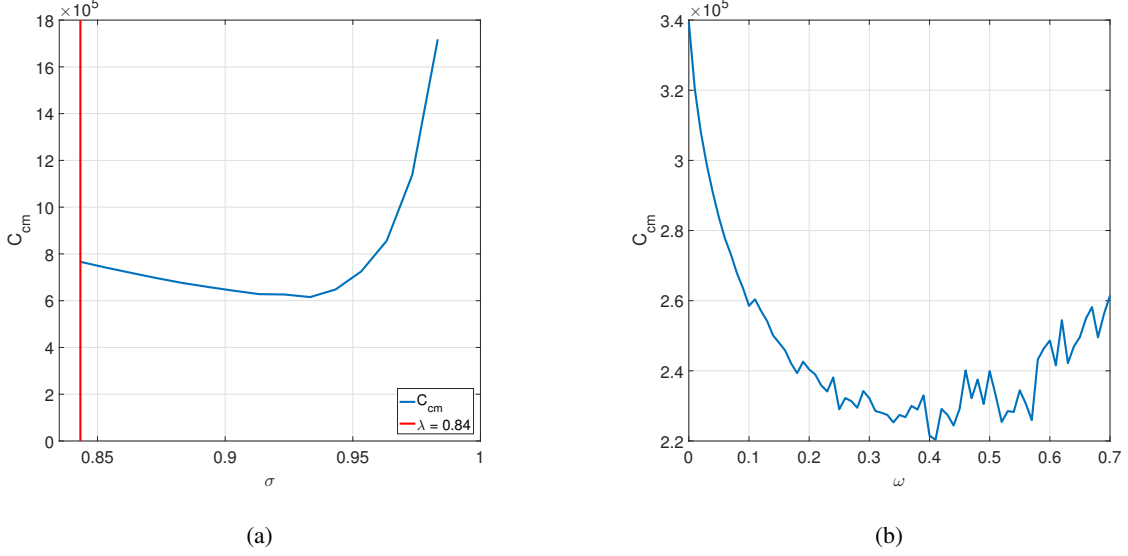


Fig. 5: Communication cost evaluation of ANQ-NIDS on smooth least square problem: (a) effect of σ with $\omega = \bar{\omega}/2$; and (b) ω with $\sigma = 0.99 \times \lambda + 0.01$.

a variety of distributed algorithms equipped with the ANQ was analyzed (in a unified fashion), showing favorable performance analytically and numerically with respect to existing quantization rules and ad-hoc distributed algorithms.

APPENDIX A

LINEAR CONVERGE UNDER QUANTIZATION

In this appendix we prove Theorem 6. We begin by introducing some preliminary results, whose proofs are deferred to Appendix A-C. Throughout this section, we make the blanket assumption that the conditions in Theorem 6 are satisfied. In particular, $\sigma \in (\lambda, 1)$ and $\omega \in [0, \bar{\omega}(\sigma))$, with $\bar{\omega}(\sigma)$ defined in (11). Due to the possibly random nature of the quantizer, $\{\mathbf{z}^k, \mathbf{c}^{k,s}, \hat{\mathbf{c}}^{k,s}\}_{k \geq 0, s \in [R]}$ is a stochastic process defined on a proper probability space; we denote by $\mathcal{F}^{k,s}$ the σ -algebra generated by $\{\mathbf{z}^{k'}, \mathbf{c}^{k',s'}, \hat{\mathbf{c}}^{k',s'}\}_{k' < k, s' \in [R]} \cup \{\mathbf{z}^k, \mathbf{c}^{k,s'}, \hat{\mathbf{c}}^{k,s'-1}\}_{s' \leq s}$ ($\hat{\mathbf{c}}^{k,s}$ excluded).

A. Preliminaries

The idea of the proof is to show by induction that both the optimization error $\|\mathbf{z}^k - \mathbf{z}^\infty\|$ and the input to the quantizer, $\|\mathbf{c}^{k,s} - \hat{\mathbf{c}}^{k-1,s}\|_2$, are linearly convergent (in expectation) at rate σ , i.e.,

$$\sqrt{\mathbb{E}[\|\mathbf{z}^k - \mathbf{z}^\infty\|^2]} \leq V_0 \cdot (\sigma)^k, \quad (29)$$

$$\sqrt{\mathbb{E}[\|\mathbf{c}^{k,s} - \hat{\mathbf{c}}^{k-1,s}\|_2^2]} \leq F^s \cdot (\sigma)^k, \quad \forall s \in [R] \cup \{0\}, \quad (30)$$

where $F^0 = 0$, and $V_0, F^s, s \in [R]$ satisfy

$$V_0 \geq \max \left\{ \|\mathbf{z}^0 - \mathbf{z}^\infty\|, \frac{\sqrt{md}R\eta^0 + \omega \mathbf{F}^\top \mathbf{1}}{\sigma - \lambda} \tilde{L}_A \right\}, \quad (31)$$

$$F^s \geq \max \left\{ L_Z c^* + L_C \sqrt{md}\eta^0 + L_C(1 + \omega)F^{s-1}, \frac{\sqrt{md}\eta^0(1 + L_C\sigma) + L_C\sigma(1 + \omega)F^{s-1} + L_Z(1 + \sigma)V_0}{\sigma - \omega} \right\}, \quad \forall s \in [R], \quad (32)$$

and we have defined $\mathbf{F} \triangleq (F^s)_{s \in [R]}$,

$$c^* \triangleq \frac{1}{L_Z} \max_{s \in [R]} \|\mathcal{C}^s(\mathbf{z}^0, \mathbf{0})\|_2, \quad (33)$$

$$\tilde{L}_A \triangleq L_A \sum_{s=0}^{R-1} (L_C)^s. \quad (34)$$

The existence of such V_0 and $F^s, s \in [R]$, is proved in the following lemma.

Lemma 16. *Let $\omega \in [0, \bar{\omega}(\sigma))$. Then, (31) and (32) are satisfied by*

$$V_0 = \max \left\{ c^*, \|\mathbf{z}^0 - \mathbf{z}^\infty\| \right\} + \frac{L_A \psi \sqrt{md} R^2 \eta^0}{\sigma - \lambda} \frac{1 + \frac{R\omega}{\sigma} [(1 + L_C\sigma)\psi - 1]}{1 - \omega/\bar{\omega}}, \quad (35)$$

$$F^s = \frac{\sqrt{md}\eta^0(1 + L_C\sigma) + 2L_Z V_0(\sigma, \omega, \eta^0)}{\sigma - \omega} \sum_{s'=0}^{s-1} \left(\frac{2L_C}{1 - \omega/\sigma} \right)^{s'}, \quad s \in [R], \quad (36)$$

where $\psi \triangleq \max\{1, (2L_C)^{R-1}\}$.

Since the effect of $\|\mathbf{c}^{k,s} - \hat{\mathbf{c}}^{k-1,s}\|_2$ on $\|\mathbf{z}^k - \mathbf{z}^\infty\|$ is through quantization, we need the following bound on the quantization error (its proof follows readily by the Cauchy–Schwarz inequality).

Lemma 17. *Let $Q_i, i \in [m]$, satisfy the BC-rule (6) with bias $\eta \geq 0$ and compression rate $\omega \in [0, \bar{\omega}(\sigma))$. Then the following holds for the stack $\mathcal{Q} \triangleq [Q_1, \dots, Q_m]^\top$:*

$$\sqrt{\mathbb{E}[\|\mathcal{Q}(\mathbf{x}) - \mathbf{x}\|_2^2]} \leq \sqrt{md}\eta + \omega \|\mathbf{x}\|_2, \quad \forall \mathbf{x} = [\mathbf{x}_1^\top, \dots, \mathbf{x}_m^\top]^\top \in \mathbb{R}^{md}. \quad (37)$$

A direct application of Lemma 17 leads to the following bound on the quantizer's input, which we use recurrently in the proofs:

$$\begin{aligned} \sqrt{\mathbb{E}[\|\hat{\mathbf{c}}^{k,s} - \mathbf{c}^{k,s}\|_2^2 | \mathcal{F}^{k,s}]} &\stackrel{(\text{Q-M})}{=} \sqrt{\mathbb{E}[\|\mathcal{Q}^k(\mathbf{c}^{k,s} - \hat{\mathbf{c}}^{k-1,s}) - (\mathbf{c}^{k,s} - \hat{\mathbf{c}}^{k-1,s})\|_2^2 | \mathcal{F}^{k,s}]} \\ &\stackrel{(37)}{\leq} \sqrt{md}\eta^0 \cdot (\sigma)^k + \omega \|\mathbf{c}^{k,s} - \hat{\mathbf{c}}^{k-1,s}\|_2, \quad a.s., \end{aligned} \quad (38)$$

for all $s \in [R]$ and $k = 0, 1, \dots$, where we used $\eta^k = \eta^0 \cdot (\sigma)^k$.

The following lemma bounds the distortion introduced by quantization in one iteration of (Q-M).

Lemma 18. *There holds: for all $k = 0, 1, \dots$,*

$$\sqrt{\mathbb{E}[\|\mathbf{z}^{k+1} - \mathbf{z}^\infty\|^2]} \leq \lambda \sqrt{\mathbb{E}[\|\mathbf{z}^k - \mathbf{z}^\infty\|^2]} + \tilde{L}_A \sqrt{mdR\eta^0} \cdot (\sigma)^k + \tilde{L}_A \omega \sum_{s=1}^R \sqrt{\mathbb{E}[\|\mathbf{c}^{k,s} - \hat{\mathbf{c}}^{k-1,s}\|_2^2]}, \quad a.s.,$$

where \tilde{L}_A is defined in (34).

We conclude this section of preliminaries with the following useful result.

Lemma 19. *Let $\{X_t : t \in [T]\} \subset \mathbb{R}$ be a collection of random variables. Then,*

$$\sqrt{\mathbb{E}\left[\left(\sum_{t=1}^T X_t\right)^2\right]} \leq \sum_{t=1}^T \sqrt{\mathbb{E}[X_t^2]}.$$

Proof. It can be proved by developing the square within the expectation on the left hand side expression, and by using $\mathbb{E}[X_t X_u] \leq \sqrt{\mathbb{E}[X_t^2]} \sqrt{\mathbb{E}[X_u^2]}$. \square

B. Proof of Theorem 6

We prove (29) and (30) by induction. Let V_0 and F^s , $s \in [R]$, satisfy (31) and (32). Since $\|\mathbf{z}^0 - \mathbf{z}^\infty\| \leq V_0$ (see (31)) and $\mathbf{c}^{0,0} = \hat{\mathbf{c}}^{-1,0} = \mathbf{0}$, (29) holds for $k = 0$ and (30) holds trivially for $k = 0$ and $s = 0$. We now use induction to prove that (30) holds for $k = 0$ and $s \in [R]$. Assume that (30) holds for $k = 0$ and $s < R$. Then, it follows that

$$\begin{aligned} \|\mathbf{c}^{0,s+1} - \hat{\mathbf{c}}^{-1,s+1}\|_2 &= \|\mathbf{c}^{0,s+1}\|_2 \\ &\stackrel{(a)}{\leq} \|\mathcal{C}^{s+1}(\mathbf{z}^0, \mathbf{0})\|_2 + \|\mathcal{C}^{s+1}(\mathbf{z}^0, \hat{\mathbf{c}}^{0,s}) - \mathcal{C}^{s+1}(\mathbf{z}^0, \mathbf{c}^{0,s})\|_2 + \|\mathcal{C}^{s+1}(\mathbf{z}^0, \mathbf{c}^{0,s}) - \mathcal{C}^{s+1}(\mathbf{z}^0, \mathbf{0})\|_2 \\ &\stackrel{(9),(33)}{\leq} L_Z c^* + L_C \|\hat{\mathbf{c}}^{0,s} - \mathbf{c}^{0,s}\|_2 + L_C \|\mathbf{c}^{0,s} - \hat{\mathbf{c}}^{-1,s}\|_2, \quad a.s., \end{aligned}$$

where in (a) we used the triangle inequality and $\mathbf{c}^{0,s+1} = \mathcal{C}^{s+1}(\mathbf{z}^0, \hat{\mathbf{c}}^{0,s})$. Taking the conditional expectation on both sides and using Lemma 19 yield

$$\begin{aligned} \sqrt{\mathbb{E}[\|\mathbf{c}^{0,s+1} - \hat{\mathbf{c}}^{-1,s+1}\|_2^2 | \mathcal{F}^{0,s}]} &\leq L_Z c^* + L_C \sqrt{\mathbb{E}[\|\hat{\mathbf{c}}^{0,s} - \mathbf{c}^{0,s}\|_2^2 | \mathcal{F}^{0,s}]} + L_C \|\mathbf{c}^{0,s} - \hat{\mathbf{c}}^{-1,s}\|_2 \\ &\stackrel{(38)}{\leq} L_Z c^* + L_C \sqrt{md\eta^0} + L_C(1 + \omega) \|\mathbf{c}^{0,s} - \hat{\mathbf{c}}^{-1,s}\|_2, \quad a.s.. \end{aligned}$$

Taking the unconditional expectation on both sides and using again Lemma 19 yield

$$\sqrt{\mathbb{E}[\|\mathbf{c}^{0,s+1} - \hat{\mathbf{c}}^{-1,s+1}\|_2^2]} \leq L_Z c^* + L_C \sqrt{md\eta^0} + L_C(1 + \omega) \sqrt{\mathbb{E}[\|\mathbf{c}^{0,s} - \hat{\mathbf{c}}^{-1,s}\|_2^2]}$$

$$\stackrel{(30)}{\leq} L_Z c^* + L_C \sqrt{m d \eta^0} + L_C (1 + \omega) F^s \stackrel{(32)}{\leq} F^{s+1},$$

which completes the induction proof of (30) for $k = 0$ and $s \in [R]$.

Now, let us assume that (29) and (30) hold for a generic $k = 0, 1, \dots$; we prove that they hold at $k + 1$. We begin with (29). Invoking Lemmata 18, 19, and using the induction hypotheses (29) and (30) at k , yield

$$\sqrt{\mathbb{E}[\|\mathbf{z}^{k+1} - \mathbf{z}^\infty\|^2]} \leq \lambda V_0 \cdot (\sigma)^k + \tilde{L}_A (\sqrt{m d R \eta^0} + \omega \mathbf{F}^\top \mathbf{1}) \cdot (\sigma)^k \leq V_0 \cdot (\sigma)^{k+1},$$

where the last inequality follows from the definition of V_0 in (31), which concludes the induction argument for (29).

We now prove that (30) holds for $k + 1$, by induction over $s \in [R]$. First, note that (30) holds trivially for $k + 1$ and $s = 0$, since $\mathbf{c}^{k+1,0} = \hat{\mathbf{c}}^{k,0} = \mathbf{0}$. Now, assume that (30) holds at iteration $k + 1$ for $s < R$. Then,

$$\begin{aligned} & \|\mathbf{c}^{k+1,s+1} - \hat{\mathbf{c}}^{k,s+1}\|_2 \stackrel{(Q-M)}{=} \|\mathcal{C}^{s+1}(\mathbf{z}^{k+1}, \hat{\mathbf{c}}^{k+1,s}) - \mathcal{C}^{s+1}(\mathbf{z}^{k+1}, \mathbf{c}^{k+1,s}) \\ & + \mathcal{C}^{s+1}(\mathbf{z}^{k+1}, \mathbf{c}^{k+1,s}) - \mathcal{C}^{s+1}(\mathbf{z}^k, \hat{\mathbf{c}}^{k,s}) + \mathbf{c}^{k,s+1} - \hat{\mathbf{c}}^{k,s+1}\|_2 \\ & \stackrel{(a)}{\leq} \|\mathcal{C}^{s+1}(\mathbf{z}^{k+1}, \hat{\mathbf{c}}^{k+1,s}) - \mathcal{C}^{s+1}(\mathbf{z}^{k+1}, \mathbf{c}^{k+1,s})\|_2 + \|\mathcal{C}^{s+1}(\mathbf{z}^{k+1}, \mathbf{c}^{k+1,s}) - \mathcal{C}^{s+1}(\mathbf{z}^k, \hat{\mathbf{c}}^{k,s})\|_2 \\ & + \|\mathbf{c}^{k,s+1} - \hat{\mathbf{c}}^{k,s+1}\|_2 \\ & \stackrel{(9),(10)}{\leq} L_C \|\hat{\mathbf{c}}^{k+1,s} - \mathbf{c}^{k+1,s}\|_2 + L_C \|\mathbf{c}^{k+1,s} - \hat{\mathbf{c}}^{k,s}\|_2 + L_Z \|\mathbf{z}^{k+1} - \mathbf{z}^\infty\|_2 \\ & + L_Z \|\mathbf{z}^k - \mathbf{z}^\infty\|_2 + \|\hat{\mathbf{c}}^{k,s+1} - \mathbf{c}^{k,s+1}\|_2, \quad a.s.. \end{aligned}$$

Then, taking the conditional expectation on $\mathcal{F}^{k+1,s}$ and invoking Lemma 19 and (38) to bound $\sqrt{\mathbb{E}[\|\hat{\mathbf{c}}^{k+1,s} - \mathbf{c}^{k+1,s}\|_2^2 | \mathcal{F}^{k+1,s}]}$, yield

$$\begin{aligned} & \sqrt{\mathbb{E}[\|\mathbf{c}^{k+1,s+1} - \hat{\mathbf{c}}^{k,s+1}\|_2^2 | \mathcal{F}^{k+1,s}]} \leq L_C \sqrt{m d \eta^0} \cdot (\sigma)^{k+1} + L_C (1 + \omega) \|\mathbf{c}^{k+1,s} - \hat{\mathbf{c}}^{k,s}\|_2 \\ & + L_Z \|\mathbf{z}^{k+1} - \mathbf{z}^\infty\|_2 + L_Z \|\mathbf{z}^k - \mathbf{z}^\infty\|_2 + \|\hat{\mathbf{c}}^{k,s+1} - \mathbf{c}^{k,s+1}\|_2, \quad a.s.. \end{aligned}$$

Now, taking the conditional expectation on $\mathcal{F}^{k,s+1} \subseteq \mathcal{F}^{k+1,s}$, invoking Lemma 19, and (38) to bound $\sqrt{\mathbb{E}[\|\hat{\mathbf{c}}^{k,s+1} - \mathbf{c}^{k,s+1}\|_2^2 | \mathcal{F}^{k,s+1}]}$, yield

$$\begin{aligned} & \sqrt{\mathbb{E}[\|\mathbf{c}^{k+1,s+1} - \hat{\mathbf{c}}^{k,s+1}\|_2^2 | \mathcal{F}^{k,s+1}]} \\ & \leq \sqrt{m d \eta^0} (1 + L_C \sigma) \cdot (\sigma)^k + L_C (1 + \omega) \sqrt{\mathbb{E}[\|\mathbf{c}^{k+1,s} - \hat{\mathbf{c}}^{k,s}\|_2^2 | \mathcal{F}^{k,s+1}]} \\ & + L_Z \sqrt{\mathbb{E}[\|\mathbf{z}^{k+1} - \mathbf{z}^\infty\|_2^2 | \mathcal{F}^{k,s+1}]} + L_Z \sqrt{\mathbb{E}[\|\mathbf{z}^k - \mathbf{z}^\infty\|_2^2 | \mathcal{F}^{k,s+1}]} + \omega \|\mathbf{c}^{k,s+1} - \hat{\mathbf{c}}^{k-1,s+1}\|_2, \quad a.s.. \end{aligned}$$

Taking the unconditional expectation and invoking Lemma 19 again yield

$$\begin{aligned}
& \sqrt{\mathbb{E}[\|\mathbf{c}^{k+1,s+1} - \hat{\mathbf{c}}^{k,s+1}\|_2^2]} \\
& \leq \sqrt{md}\eta^0(1 + L_C\sigma) \cdot (\sigma)^k + L_C(1 + \omega)\sqrt{\mathbb{E}[\|\mathbf{c}^{k+1,s} - \hat{\mathbf{c}}^{k,s}\|_2^2]} \\
& + L_Z\sqrt{\mathbb{E}[\|\mathbf{z}^{k+1} - \mathbf{z}^\infty\|_2^2]} + L_Z\sqrt{\mathbb{E}[\|\mathbf{z}^k - \mathbf{z}^\infty\|_2^2]} + \omega\sqrt{\mathbb{E}[\|\mathbf{c}^{k,s+1} - \hat{\mathbf{c}}^{k-1,s+1}\|_2^2]} \\
& \stackrel{(a)}{\leq} \sqrt{md}\eta^0(1 + L_C\sigma) \cdot (\sigma)^k + L_C(1 + \omega)F^s \cdot (\sigma)^{k+1} + \omega F^{s+1} \cdot (\sigma)^k + L_Z(1 + \sigma)V_0 \cdot (\sigma)^k \\
& \stackrel{(32)}{\leq} F^{s+1} \cdot (\sigma)^{k+1},
\end{aligned}$$

where in (a) we used the induction hypotheses (30) (applied to the second and last terms) and (29) (applied to the third and fourth terms). This proves the induction for (30), and the theorem.

C. Proof of auxiliary lemmata for Theorem 6

1) Proof of Lemma 16: It is not difficult to check that conditions (31) and (32) can be satisfied by choosing

$$\begin{aligned}
V_0 & \geq \max \left\{ c^*, \|\mathbf{z}^0 - \mathbf{z}^\infty\|, \frac{\sqrt{md}R\eta^0 + \omega\mathbf{F}^\top \mathbf{1}}{\sigma - \lambda} \tilde{L}_A \right\}, \\
F^s & \geq \frac{\sqrt{md}\eta^0(1 + L_C\sigma) + L_C\sigma(1 + \omega)F^{s-1} + L_Z(1 + \sigma)V_0}{\sigma - \omega}, \quad \forall s \in [R],
\end{aligned}$$

where c^* , \tilde{L}_A are defined in (33) and (34), respectively. Moreover, since $\omega < \sigma < 1$, it is sufficient to choose

$$F^s = \frac{1}{\sigma} \frac{\sqrt{md}\eta^0(1 + L_C\sigma) + 2L_C\sigma F^{s-1} + 2L_ZV_0}{1 - \omega/\sigma}, \quad \forall s \in [R].$$

Solving this expression recursively yields (36).

We now prove (35). We begin noting that F^s is a non-decreasing function of s , hence $F^s \leq F^R$. Moreover, F^R is an affine function of V_0 . Using the facts that $(\frac{2L_C}{1-\omega/\sigma})^s \leq \psi(1 - \omega/\sigma)^{-s}$, where $\psi \triangleq \max\{1, (2L_C)^{R-1}\}$, and $(1 - \omega/\sigma)^{-s} \leq (1 - \omega/\sigma)(1 - R\omega/\sigma)^{-1}$, for all $s \in [R - 1] \cup \{0\}$ and $\omega < \bar{\omega}(\sigma) < \sigma/R$, we can upper bound F^s as

$$F^s \leq F^R \leq a_1 + V_0 a_2 \triangleq \bar{F}^R, \tag{39}$$

where

$$a_1 \triangleq \psi \sqrt{md}\eta^0(1 + L_C\sigma) \cdot \frac{R/\sigma}{1 - R\omega/\sigma}, \tag{40}$$

$$a_2 \triangleq 2L_Z\psi \cdot \frac{R/\sigma}{1 - R\omega/\sigma}. \tag{41}$$

Furthermore, since $\mathbf{F}^\top \mathbf{1} \leq RF^R \leq R(a_1 + V_0 a_2)$ and $\tilde{L}_A = L_A \sum_{s=0}^{R-1} (L_C)^s \leq L_A \psi R$, to satisfy (31), it is sufficient to choose V_0 as

$$V_0 \geq \max \left\{ c^*, \|\mathbf{z}^0 - \mathbf{z}^\infty\|, L_A \psi R^2 \frac{\sqrt{md}\eta^0 + \omega(a_1 + V_0 a_2)}{\sigma - \lambda} \right\}.$$

Using $x \geq \max\{c, a + bx\} \Leftrightarrow x \geq \max\{c, a/(1-b)\}$, under $b < 1$, the above condition is equivalent to

$$V_0 \geq \max \left\{ c^*, \|\mathbf{z}^0 - \mathbf{z}^\infty\|, \frac{L_A \psi R^2 (\sqrt{md}\eta^0 + \omega a_1)}{\sigma - \lambda - L_A \psi R^2 \omega a_2} \right\}, \quad (42)$$

as long as $L_A \psi R^2 \omega a_2 / (\sigma - \lambda) < 1$. Solving with respect to ω (note that a_2 is a function of ω), this condition is equivalent to $\omega \in [0, \bar{\omega}(\sigma))$ with $\bar{\omega}(\sigma)$ given by (11), hence it holds by assumption. Substituting the values of a_1, a_2 in (42) and using $\max\{a, b\} \leq a + b$ (for $a, b \geq 0$), yields (35). \square .

2) Proof of Lemma 18: At iteration k , let ζ_s be defined as

$$\zeta^s = \mathcal{A}(\mathbf{z}^k, \hat{\mathbf{c}}^{k,1}, \dots, \hat{\mathbf{c}}^{k,s}, \tilde{\mathbf{c}}_s^{s+1}, \dots, \tilde{\mathbf{c}}_s^R),$$

where

$$\tilde{\mathbf{c}}_s^s = \hat{\mathbf{c}}^{k,s} \quad \text{and} \quad \tilde{\mathbf{c}}_s^{\ell+1} \triangleq \mathcal{C}^{\ell+1}(\mathbf{z}^k, \tilde{\mathbf{c}}_s^\ell), \forall \ell \geq s.$$

In other words, $\tilde{\mathbf{c}}_s^\ell, \zeta^s$ are the communication signals at round ℓ and the updated computation state, respectively, obtained by applying the unquantized communication mapping after round s and the quantized one before round s . Clearly, $\mathbf{z}^{k+1} = \mathcal{A}(\mathbf{z}^k, \hat{\mathbf{c}}^{k,1}, \dots, \hat{\mathbf{c}}^{k,R}) = \zeta^R$ and $\tilde{\mathcal{A}}(\mathbf{z}^k) = \zeta^0$ (unquantized update of the computation state). It then follows that

$$\mathbf{z}^{k+1} = \zeta^R = \tilde{\mathcal{A}}(\mathbf{z}^k) + \sum_{s=1}^R (\zeta^s - \zeta^{s-1}), \quad a.s..$$

Invoking the triangle inequality yields

$$\|\mathbf{z}^{k+1} - \mathbf{z}^\infty\| \leq \|\tilde{\mathcal{A}}(\mathbf{z}^k) - \mathbf{z}^\infty\| + \sum_{s=1}^R \|\zeta^s - \zeta^{s-1}\|, \quad a.s.. \quad (43)$$

We now study the second term. From the Lipschitz continuity of \mathcal{A} (Assumption 4) and the definition of ζ^s , it holds that

$$\|\zeta^s - \zeta^{s-1}\| \leq L_A \sum_{\ell=s}^R \|\tilde{\mathbf{c}}_s^\ell - \tilde{\mathbf{c}}_{s-1}^\ell\|_2, \quad a.s..$$

Furthermore, $\|\tilde{\mathbf{c}}_s^s - \tilde{\mathbf{c}}_{s-1}^s\|_2 = \|\hat{\mathbf{c}}^{k,s} - \mathcal{C}^s(\mathbf{z}^k, \hat{\mathbf{c}}^{k,s-1})\|_2 = \|\hat{\mathbf{c}}^{k,s} - \mathbf{c}^{k,s}\|_2$ a.s., and, for $\ell > s$,

$$\|\tilde{\mathbf{c}}_s^\ell - \tilde{\mathbf{c}}_{s-1}^\ell\|_2 = \|\mathcal{C}^\ell(\mathbf{z}^k, \tilde{\mathbf{c}}_s^{\ell-1}) - \mathcal{C}^\ell(\mathbf{z}^k, \tilde{\mathbf{c}}_{s-1}^{\ell-1})\|_2 \leq L_C \|\tilde{\mathbf{c}}_s^{\ell-1} - \tilde{\mathbf{c}}_{s-1}^{\ell-1}\|_2 \leq \dots \leq (L_C)^{\ell-s} \|\hat{\mathbf{c}}^{k,s} - \mathbf{c}^{k,s}\|_2,$$

a.s., where the last step follows from induction over ℓ . Replacing these bounds in (43), we finally obtain

$$\begin{aligned} \|\mathbf{z}^{k+1} - \mathbf{z}^\infty\| &\leq \|\tilde{\mathcal{A}}(\mathbf{z}^k) - \mathbf{z}^\infty\| + L_A \sum_{s=1}^R \sum_{\ell=0}^{R-s} (L_C)^\ell \|\hat{\mathbf{c}}^{k,s} - \mathbf{c}^{k,s}\|_2 \\ &\leq \lambda \|\mathbf{z}^k - \mathbf{z}^\infty\| + \tilde{L}_A \sum_{s=1}^R \|\hat{\mathbf{c}}^{k,s} - \mathbf{c}^{k,s}\|_2, \quad a.s., \end{aligned}$$

where \tilde{L}_A is defined in (34) and we used Assumption 1. Taking the conditional expectation on the filtration $\mathcal{F}^{k,s}$ while applying Lemma 19 and (38), starting from $s = R, R-1, \dots, 1$, it follows that

$$\begin{aligned} &\sqrt{\mathbb{E}[\|\mathbf{z}^{k+1} - \mathbf{z}^\infty\|^2 | \mathcal{F}^{k,1}]} \\ &\leq \lambda \|\mathbf{z}^k - \mathbf{z}^\infty\| + \tilde{L}_A \sqrt{mdR\eta^0} \cdot (\sigma)^k + \tilde{L}_A \omega \sum_{s=1}^R \sqrt{\mathbb{E}[\|\mathbf{c}^{k,s} - \hat{\mathbf{c}}^{k-1,s}\|_2^2 | \mathcal{F}^{k,1}]}, \quad a.s.. \end{aligned}$$

Finally, taking unconditional expectation and using Lemma 19 concludes the proof.

APPENDIX B

DETERMINISTIC AND RANDOM QUANTIZER'S DESIGN

A. Proof of Lemma 7

Let $\mathcal{Q}(\bullet) : [-\delta, \delta]^d \rightarrow \mathbb{Q}^d$ be a component-wise quantizer, with the n th quantizer $\mathcal{Q}_n(\bullet)$ mapping points in the interval $[-\delta, \delta]$ to quantization points in the set \mathbb{Q} (we assume that the same quantizer is applied across all n , since each component is optimized with the same range and number of quantization points). The goal is to define a quantizer \mathcal{Q} which satisfies the BC-rule within $\mathbf{x} \in [-\delta, \delta]^d$ with maximal range δ . To this end, note that a necessary and sufficient condition is

$$|\mathcal{Q}_n(x) - x| \leq \eta + \omega|x|, \quad \forall x \in [-\delta, \delta], \quad \forall n \in [d]. \quad (44)$$

The sufficiency can be proved using Cauchy–Schwarz inequality. To prove the necessity, assume that (44) is violated for some $x \in [-\delta, \delta]$, i.e., $|\mathcal{Q}_n(x) - x| > \eta + \omega|x|$, and let $\mathbf{x} = x\mathbf{1}$. It follows that

$$\|\mathcal{Q}(\mathbf{x}) - \mathbf{x}\|_2 = \sqrt{d}|\mathcal{Q}_n(x) - x| > \sqrt{d}\eta + \omega\sqrt{d}|x| = \sqrt{d}\eta + \omega\|\mathbf{x}\|_2,$$

implying the BC-rule is not satisfied at \mathbf{x} .

Hence, we now focus on the design of a component-wise quantizer \mathcal{Q}_n satisfying (44) with maximal range δ . In the following, we omit the dependence on n for convenience.

Assume that $N = |\mathbb{Q}|$ is odd (the case N even can be studied in a similar fashion, and is provided at the end of this proof for completeness), and let $\mathbb{Q} \triangleq \cup_{\ell=0}^{(N-1)/2} \{\tilde{q}_\ell, -\tilde{q}_\ell\}$ be the set of quantization points, with $0 = \tilde{q}_0 < \tilde{q}_1 < \dots, \tilde{q}_\ell < \tilde{q}_{\ell+1} < \dots$. Note that we restrict to a symmetric quantizer since the error metric is symmetric around 0 (the detailed proof on the optimality of symmetric quantizers is omitted due to space constraints). We then aim to solve

$$\begin{aligned} & \max_{\delta \geq 0, \mathbb{Q}} && \delta \\ \text{s.t.} & && |\mathcal{Q}(x) - x| \leq \eta + \omega x, \quad \forall x \in [0, \delta], \end{aligned} \quad (45)$$

where the constraint (44) is imposed only to $x \in [0, \delta]$ since the quantizer is symmetric around 0. Since the quantization error in (45) is measured in Euclidean distance, it is optimal to restrict the quantization points to $\mathbb{Q} \subset [-\delta, \delta]$ and to map the input to the nearest quantization point (ties may be resolved arbitrarily). Then, letting $\mathcal{X}_\ell = ((\tilde{q}_{\ell-1} + \tilde{q}_\ell)/2, (\tilde{q}_\ell + \tilde{q}_{\ell+1})/2]$, with $\tilde{q}_{-1} = 0$ and $\tilde{q}_{(N+1)/2} = 2\delta - \tilde{q}_{(N-1)/2}$, it follows that $[0, \delta] \equiv \cup_{\ell=0}^{(N-1)/2} \mathcal{X}_\ell$ and $\mathcal{Q}(x) = \tilde{q}_\ell, \forall x \in \mathcal{X}_\ell$. Therefore, the optimization problem (45) can be expressed equivalently as

$$\begin{aligned} & \max_{\delta \geq 0, \tilde{\mathbf{q}}} && \delta \\ \text{s.t.} & && (\tilde{q}_\ell - x)^2 \leq (\eta + \omega x)^2, \quad \forall x \in \mathcal{X}_\ell, \quad \forall \ell = 0, 1, \dots, (N-1)/2, \\ & && 0 = \tilde{q}_0 \leq \dots \leq \tilde{q}_{(N+1)/2} = 2\delta - \tilde{q}_{(N-1)/2}. \end{aligned}$$

Equivalently,

$$\begin{aligned} & \max_{\delta \geq 0, \tilde{\mathbf{q}}} && \delta \\ \text{s.t.} & && \max_{x \in \mathcal{X}_\ell} (\tilde{q}_\ell - x)^2 - (\eta + \omega x)^2 \leq 0, \quad \forall \ell = 0, 1, \dots, (N-1)/2, \\ & && 0 = \tilde{q}_0 \leq \dots \leq \tilde{q}_{(N+1)/2} = 2\delta - \tilde{q}_{(N-1)/2}, \end{aligned}$$

and solving the maximization with respect to $x \in \mathcal{X}_\ell$ (note that the quadratic function is convex in x , hence it is maximized at the margins of \mathcal{X}_ℓ), we obtain

$$\begin{aligned} & \max_{\delta \geq 0, \tilde{\mathbf{q}}} && \frac{\tilde{q}_{(N-1)/2} + \tilde{q}_{(N+1)/2}}{2} \\ \text{s.t.} & && \tilde{q}_\ell \leq \tilde{q}_{\ell-1} \left(\frac{1+\omega}{1-\omega} \right) + \frac{2\eta}{1-\omega}, \quad \forall \ell \in [(N+1)/2], \\ & && 0 = \tilde{q}_0 < \tilde{q}_1 < \dots < \tilde{q}_{(N+1)/2}. \end{aligned}$$

Solving this problem with respect to $\tilde{\mathbf{q}}$ yields $q_0 = 0$ and

$$q_\ell = q_{\ell-1} \left(\frac{1+\omega}{1-\omega} \right) + \frac{2\eta}{1-\omega}, \quad \forall \ell \geq 1.$$

Solving by induction, we obtain q_ℓ as in (13), $\delta(\eta, \omega, N)$ as in (12), and

$$\ell(x) = \text{sign}(x) \cdot \min \left\{ \ell \geq 0 : \frac{q_\ell + q_{\ell+1}}{2} \geq |x| \right\},$$

yielding (14) after solving with the expression of q_ℓ . A similar technique can be proved for the case when N is even. In this case, the quantization points are given by

$$q_\ell = -q_{-\ell} = \frac{\eta}{\omega} \left[\frac{(1 + \omega)^\ell}{(1 - \omega)^{\ell-1}} - 1 \right], \quad \forall \ell \geq 1$$

and $\delta(\eta, \omega, N) = (q_{N/2} + q_{N/2+1})/2$, which concludes the proof.

B. Proof of Lemma 8

Using a similar technique as in Appendix B-A when N is odd, using the fact that $[0, \delta] = \cup_{\ell \in [(N-1)/2]} [\tilde{q}_{\ell-1}, \tilde{q}_\ell]$ and $\delta = \tilde{q}_{N/2}$ it suffices to solve

$$\begin{aligned} & \max_{\delta \geq 0, \tilde{\mathbf{q}}} && q_{(N-1)/2} \\ \text{s.t.} & && \mathbb{E}[|\mathcal{Q}(x) - x|^2] \leq (\eta + \omega x)^2, \quad \forall x \in [\tilde{q}_{\ell-1}, \tilde{q}_\ell], \quad \forall \ell = [(N-1)/2], \\ & && \mathbb{E}[\mathcal{Q}(x)] = x, \quad 0 = \tilde{q}_0 \leq \dots \leq \tilde{q}_{(N-1)/2} = \delta. \end{aligned}$$

Furthermore, since $x \in [\tilde{q}_{\ell-1}, \tilde{q}_\ell]$ is mapped to $\tilde{q}_{\ell-1}$ w.p. $(\tilde{q}_\ell - x)/(\tilde{q}_\ell - \tilde{q}_{\ell-1})$ and to \tilde{q}_ℓ w.p. $(x - \tilde{q}_{\ell-1})/(\tilde{q}_\ell - \tilde{q}_{\ell-1})$ to satisfy $\mathbb{E}[\mathcal{Q}(x)] = x$, the problem can be expressed equivalently as

$$\begin{aligned} & \max_{\delta \geq 0, \tilde{\mathbf{q}}} && q_{(N-1)/2} \\ \text{s.t.} & && (x - \tilde{q}_\ell)(x - \tilde{q}_{\ell-1}) + (\eta + \omega x)^2 \geq 0, \quad \forall x \in [\tilde{q}_{\ell-1}, \tilde{q}_\ell], \quad \forall \ell = [(N-1)/2], \\ & && 0 = \tilde{q}_0 \leq \dots \leq \tilde{q}_{(N-1)/2} = \delta, \end{aligned}$$

or equivalently

$$\begin{aligned} & \max_{\delta \geq 0, \tilde{\mathbf{q}}} && q_{(N-1)/2} \\ \text{s.t.} & && \min_{x \in [\tilde{q}_{\ell-1}, \tilde{q}_\ell]} (x - \tilde{q}_\ell)(x - \tilde{q}_{\ell-1}) + (\eta + \omega x)^2 \geq 0, \quad \forall \ell = [(N-1)/2], \\ & && 0 = \tilde{q}_0 \leq \dots \leq \tilde{q}_{(N-1)/2} = \delta. \end{aligned}$$

Solving the minimization over $x \in [\tilde{q}_{\ell-1}, \tilde{q}_\ell]$ and solving with respect to $\tilde{\mathbf{q}}$ yields the following optimal quantization points: $q_0 = 0$ and

$$q_\ell = q_{\ell-1}(\sqrt{1 + (\omega)^2} + \omega)^2 + 2\eta(\sqrt{1 + (\omega)^2} + \omega), \quad \forall \ell \geq 1.$$

Solving by induction, we obtain q_ℓ as in (16), $\delta(\eta, \omega, N)$ as in (15), and the probabilistic quantization rule as in (17), with ℓ given by

$$\ell = \text{sign}(x) \cdot \min \left\{ \ell \geq 0 : q_\ell \geq |x| \right\},$$

yielding (17) after solving with the expression of q_ℓ .

A similar technique can be proved for the case when N is even. In this case, the quantization points are given by

$$q_\ell = \frac{\eta}{\omega} \left[\frac{(\sqrt{1 + (\omega)^2} + \omega)^{2\ell-1}}{\sqrt{1 + (\omega)^2}} - 1 \right], \quad \forall \ell \geq 1.$$

and $\delta(\eta, \omega, N) = q_{N/2}$, which concludes the proof.

C. Proof of Corollary 9

Let $\mathcal{Q}(\mathbf{x})$ be a generic deterministic or probabilistic quantizer with domain $[-\delta, \delta]^d$ and codomain $\mathbb{Q} \in \mathbb{R}^d$ with $|\mathbb{Q}| < \infty$, that satisfies the BC-rule with $\eta = 0$. It follows that

$$\omega \|\mathbf{x}\|_2 \geq \sqrt{\mathbb{E}[\|\mathcal{Q}(\mathbf{x}) - \mathbf{x}\|_2^2]} \geq \min_{\mathbf{q} \in \mathbb{Q}} \|\mathbf{q} - \mathbf{x}\|_2 = \|\mathcal{Q}_{\text{det}}(\mathbf{x}) - \mathbf{x}\|_2, \quad \forall \mathbf{x} \in [-\delta, \delta]^d, \quad (46)$$

where the lower bound is achievable by a deterministic quantizer that maps \mathbf{x} to the nearest quantization point, denoted as $\mathcal{Q}_{\text{det}}(\mathbf{x})$. Let $\mathcal{Q}_n(x) = \mathbf{e}_n^\top \mathcal{Q}_{\text{det}}(x\mathbf{e}_n)$ be the projection of \mathcal{Q}_{det} on its n th element, where \mathbf{e}_n is the n th canonical vector. Since $\|\mathcal{Q}_{\text{det}}(x\mathbf{e}_n) - x\mathbf{e}_n\|_2 \geq |\mathcal{Q}_n(x) - x|$, from (46) it follows that

$$\omega \|x\mathbf{e}_n\|_2 = \omega |x| \geq \|\mathcal{Q}_{\text{det}}(x\mathbf{e}_n) - x\mathbf{e}_n\|_2 \geq |\mathcal{Q}_n(x) - x|, \quad \forall x \in [-\delta, \delta],$$

hence \mathcal{Q}_n satisfies the BC-rule with $\eta = 0$ as well. Note that \mathcal{Q}_n is a scalar quantizer with $N_n \leq |\mathbb{Q}|$ quantization points. However, Lemma 7 dictates that $\delta = 0$ for this quantizer, hence the contradiction, and we have proved the statement for both deterministic and probabilistic compression rules.

APPENDIX C

COMMUNICATION COST ANALYSIS

A. Proof of Theorem 12

We first present some preliminary results instrumental to prove Theorem 12, whose proofs are deferred to Appendix C-B.

The idea of the proof is to study the asymptotic behavior of an upper bound on the number of bits required per iteration, provided in the following lemma.

Lemma 20. *Under the same setting as Theorem 6, and the proposed ANQ satisfying the BC rule, the average number of bits required per agent at the k th iteration, B^k , is upper bounded as*

$$\mathbb{E}[B^k] \leq \log_2(S+1) \left[3dR + dR \log_S \left(3 + \frac{\bar{F}^R(\sigma, \omega, \eta^0)}{\sqrt{md}\eta^0} \right) \right] \text{ bits}, \quad \forall k \geq 0, \quad (47)$$

where $\bar{F}^R(\sigma, \omega, \eta^0)$ is defined in (39).

In addition, we need the following lemma to connect the asymptotic results of the logarithmic function and its argument.

Lemma 21. *For positive functions f, g , it holds: $\ln f(x) = \mathcal{O}(\ln g(x))$ as $x \rightarrow x_0$ if $\liminf_{x \rightarrow x_0} g(x) > 1$, and $f(x) = \mathcal{O}(g(x))$ as $x \rightarrow x_0$.*

We are now ready to prove the main theorem. From Lemma 20, the average number of bits per agent per iteration is upper bounded by

$$\mathbb{E}[B_k] \leq \log_2(S+1) \left[3dR + dR \log_S \left(3 + \frac{\bar{F}^R(\sigma, \omega, \eta^0)}{\sqrt{md}\eta^0} \right) \right], \quad \forall k = 0, 1, \dots,$$

where

$$\bar{F}^R(\sigma, \omega, \eta^0) = a_1 + a_2 V_0,$$

a_1 and a_2 are defined in (40) and (41), respectively; and V_0 is given in (35). We want to prove that this is $\mathbb{E}[B_k] = \mathcal{O}(d \ln(1 + \frac{1}{\sigma(\sigma-\lambda)}))$ under Assumption 11 and conditions $\eta^0 = \Theta(L_Z(\sigma - \lambda))$, $1 - \omega/\bar{\omega}(\sigma) = \Omega(1)$. Using the fact that $\bar{F}^R(\sigma, \omega, \eta^0)/\eta^0 = a_1/\eta^0 + a_2 V_0/\eta^0$, it is sufficient to show that $a_1/(\sqrt{md}\eta^0) = \mathcal{O}(1 + \frac{1}{\sigma})$ and $a_2 V_0/(\sqrt{md}\eta^0) = \mathcal{O}(1 + \frac{1}{\sigma(\sigma-\lambda)})$. In fact, using $R/\sigma \leq 1/\bar{\omega}(\sigma)$, we can bound a_1 and a_2 as

$$\begin{aligned} a_1/(\sqrt{md}\eta^0) &\leq \frac{1}{\sigma} (1 + L_C \sigma) \max\{1, (2L_C)^{R-1}\} \frac{R}{1 - \omega/\bar{\omega}(\sigma)}, \\ a_2 &\leq \frac{2L_Z}{\sigma} \max\{1, (2L_C)^{R-1}\} \frac{R}{1 - \omega/\bar{\omega}(\sigma)}. \end{aligned}$$

Clearly, $a_1/(\sqrt{md}\eta^0) = \mathcal{O}(1 + \frac{1}{\sigma})$ and $a_2 = \mathcal{O}(\frac{L_Z}{\sigma})$ since $L_C, R = \mathcal{O}(1)$ and $1 - \omega/\bar{\omega}(\sigma) = \Omega(1)$. We next study V_0 . From its expression in (35), we notice that $V_0 = \mathcal{O}(\sqrt{md})$ since $\omega/\sigma \leq 1$, $\max\{c^*, \|\mathbf{z}^0 - \mathbf{z}^\infty\|_2\} = \mathcal{O}(\sqrt{md})$, $\eta^0 = \Theta(L_Z(\sigma - \lambda))$, $L_A L_Z, L_C, R = \mathcal{O}(1)$, and $1 - \omega/\bar{\omega} = \Omega(1)$. Therefore, it follows that $a_2 V_0/(\sqrt{md}\eta^0) = \mathcal{O}(\frac{1}{\sigma(\sigma-\lambda)}) = \mathcal{O}(1 + \frac{1}{\sigma(\sigma-\lambda)})$, and the proof is completed by invoking Lemma 21.

B. Auxiliary results for Theorem 12

1) Proof of Lemma 20: Let $\Delta \mathbf{c}_i^{k,s} \triangleq \mathbf{c}_i^{k,s} - \hat{\mathbf{c}}_i^{k-1,s}$ be the input to the quantizer for agent i , at iteration k and communication round s . We now study the average number of bits required for 1) the deterministic quantizer, and 2) the probabilistic quantizer with $\mathbb{E}[\mathcal{Q}(x)] = x$.

i) Deterministic quantizer: The average number of bits required is bounded as (see (19)), one can also verify that the following also holds for even N)

$$b_i^{k,s} \leq \log_2(S+1) \left[3d + d \log_S \left(2 + \frac{\ln \left(1 + \frac{\omega \|\Delta \mathbf{c}_i^{k,s}\|_2}{\sqrt{d} \eta^0 \cdot (\sigma)^k} \right)}{\ln(1+\omega) - \ln(1-\omega)} \right) \right] \text{ bits.}$$

We now upper bound the argument inside the second logarithm. Since it is a decreasing function of ω , it is maximized in the limit $\omega \rightarrow 0$, yielding

$$\frac{\ln \left(1 + \frac{\omega \|\Delta \mathbf{c}_i^{k,s}\|_2}{\sqrt{d} \eta^0 \cdot (\sigma)^k} \right)}{\ln(1+\omega) - \ln(1-\omega)} \leq \frac{\|\Delta \mathbf{c}_i^{k,s}\|_2}{2\sqrt{d} \eta^0 \cdot (\sigma)^k}.$$

With this upper bound, we can then upper bound the average number of bits per agent at communication round s , iteration k , as

$$\begin{aligned} \mathbb{E}[b^{k,s}] &\triangleq \frac{1}{m} \sum_{i=1}^m \mathbb{E}[b_i^{k,s}] \stackrel{(a)}{\leq} \log_2(S+1) \left[3d + d \log_S \left(2 + \frac{\sqrt{\mathbb{E}[\|\mathbf{c}^{k,s} - \hat{\mathbf{c}}^{k-1,s}\|_2^2]}}{2\sqrt{m} d \eta^0 \cdot (\sigma)^k} \right) \right] \\ &\stackrel{(b)}{\leq} \log_2(S+1) \left[3d + d \log_S \left(2 + \frac{F^s(\sigma, \omega, \eta^0)}{2\sqrt{m} d \eta^0} \right) \right] \\ &\stackrel{(c)}{\leq} \log_2(S+1) \left[3d + d \log_S \left(2 + \frac{\bar{F}^R(\sigma, \omega, \eta^0)}{2\sqrt{m} d \eta^0} \right) \right], \end{aligned}$$

where (a) follows from Cauchy–Schwarz inequality, Jensen’s inequality, and the definition of $\Delta \mathbf{c}^{k,s}$; (b) follows from (30); and (c) follows from $F^s \leq \bar{F}^R$ (see (39)).

ii) Probabilistic quantizer with $\mathbb{E}[\mathcal{Q}(x)] = x$: Using the same technique as in i), along with the inequality $1 - 1/x \leq \ln(x) \leq x - 1$ for $x > 1$ to bound the argument inside the second logarithm of (20),

$$\mathbb{E}[b^{k,s}] \leq \log_2(S+1) \left[3d + d \log_S \left(3 + \frac{\bar{F}^R(\sigma, \omega, \eta^0)}{\sqrt{m} d \eta^0} \right) \right].$$

One can also verify that it also holds for even N .

Finally, for both the deterministic and probabilistic cases, the proof is completed by summing over $s \in [R]$ to get the average communication cost per agent at iteration k .

2) Proof of Lemma 21: If $f(x) = \mathcal{O}(g(x))$ as $x \rightarrow x_0$ and $\liminf_{x \rightarrow x_0} g(x) > 1$, then

$$\limsup_{x \rightarrow x_0} \left| \frac{\ln f(x)}{\ln g(x)} \right| \leq 1 + \limsup_{x \rightarrow x_0} \left| \frac{\ln(f(x)/g(x))}{\ln g(x)} \right| \stackrel{(a)}{\leq} 1 + \frac{\limsup_{x \rightarrow x_0} |\ln(f(x)/g(x))|}{|\liminf_{x \rightarrow x_0} \ln g(x)|} < \infty,$$

where (a) follows from $\liminf_{x \rightarrow x_0} g(x) > 1$. This completes the proof.

C. Proof of Theorem 13

Since $\sqrt{\mathbb{E}[\|\mathbf{z}^k - \mathbf{z}^\infty\|^2]} \leq V_0 \cdot (\sigma)^k$ (cf. Theorem 6), the ε -accuracy is achieved if $k[-\ln(\sigma)] \geq \ln(V_0/\sqrt{m\varepsilon})$, which yields $k(1-\sigma) \geq \ln(V_0/\sqrt{m\varepsilon})$ since $-\ln(\sigma) \geq 1-\sigma$. Hence, ε -accuracy is achieved if all conditions in Theorem 6 hold and $k \geq k_\varepsilon \triangleq \lceil \frac{1}{1-\sigma} \ln \frac{V_0}{\sqrt{m\varepsilon}} \rceil$. Hence, to compute the upper bound of the communication cost $\sum_{k=0}^{k_\varepsilon-1} \mathbb{E}[B^k]$, we need the upper bounds for $\mathbb{E}[B^k]$, $\frac{1}{1-\sigma}$ and V_0 . In the proof of Theorem 12, we found that, under Assumption 11 and the conditions $1 - \omega/\bar{\omega}(\sigma) = \Omega(1), \eta^0 = \Theta(L_Z(\sigma - \lambda))$,

$$\mathbb{E}[B^k] = \mathcal{O}\left(d \log_2 \left(1 + \frac{1}{\sigma(\sigma - \lambda)}\right)\right), \quad V_0 = \mathcal{O}(\sqrt{md}).$$

Moreover, it can be shown that $1/\sigma \leq \frac{(1-\lambda)^2}{(1-\sigma)(\sigma-\lambda)}$ for $\sigma \in (\lambda, 1)$, and therefore

$$\frac{1}{\sigma(\sigma - \lambda)} \leq \frac{1}{(1-\lambda)} \left[\frac{(1-\lambda)^2}{(1-\sigma)(\sigma-\lambda)} \right]^2 \frac{1-\sigma}{1-\lambda} = \mathcal{O}\left(\frac{1}{1-\lambda}\right),$$

where we used $\frac{(1-\lambda)^2}{(1-\sigma)(\sigma-\lambda)} = \mathcal{O}(1)$. It then follows from Lemma 21 that $\mathbb{E}[B^k] = \mathcal{O}(d \log_2(1 + \frac{1}{1-\lambda}))$. On the other hand, we can bound k_ε as

$$k_\varepsilon \leq \frac{1}{1-\lambda} \left(1 - \lambda + \frac{1-\lambda}{1-\sigma} \log_2 \frac{V_0}{\sqrt{m\varepsilon}}\right) = \mathcal{O}\left(\frac{1}{1-\lambda} \log_2 \left(\frac{d}{\varepsilon}\right)\right),$$

since $\frac{1-\lambda}{1-\sigma} = \mathcal{O}(1)$ and $V_0 = \mathcal{O}(\sqrt{md})$. Therefore, the communication cost satisfies

$$\sum_{k=0}^{k_\varepsilon-1} \mathbb{E}[B^k] = \mathcal{O}\left(d k_\varepsilon \log_2 \left(1 + \frac{1}{1-\lambda}\right)\right) = \mathcal{O}\left(\frac{d}{1-\lambda} \log_2 \left(\frac{d}{\varepsilon}\right) \log_2 \left(1 + \frac{1}{1-\lambda}\right)\right),$$

which completes the proof.

D. Proof of Lemma 10

Consider $\ell \geq 0$. Using (18), the number of information symbols required to encode ℓ is

$$b_\ell^* = \min \left\{ b \geq 0 : \ell \leq \left\lfloor \frac{(S)^{b+1} - 1}{2(S-1)} \right\rfloor \right\}.$$

Similarly, for $\ell < 0$,

$$b_\ell^* = \min \left\{ b \geq 0 : -\ell \leq \left\lceil \frac{(S)^{b+1} - 1}{2(S-1)} \right\rceil - 1 \right\}.$$

Since $\lfloor \frac{(S)^{b+1}-1}{2(S-1)} \rfloor \geq \lceil \frac{(S)^{b+1}-1}{2(S-1)} \rceil - 1 \geq \frac{(S)^{b+1}-1}{2(S-1)} - 1$, we can then upper bound $b_\ell, \ell \in \mathbb{Z}$, as

$$\begin{aligned} b_\ell^* &\leq \min\{b \geq 1 : 1 + 2(S-1)(1 + |\ell|) \leq (S)^{b+1}\} \\ &= \min\{b \geq 1 : b \geq \log_S(2 - 1/S + 2(1 - 1/S)|\ell|)\} = \lceil \log_S(2 - 1/S + 2(1 - 1/S)|\ell|) \rceil. \end{aligned}$$

Using $\lceil x \rceil \leq x + 1$ We can then further upper bound

$$b_\ell^* \leq 1 + \log_S(2 - 1/S + 2(1 - 1/S)|\ell|) \leq \log_S(2S + 2S|\ell|) \leq 2 + \log_S(1 + |\ell|),$$

resulting the upper bound to the communication cost (including the termination symbol)

$$\bar{C}_{\text{comm}}(\ell) \leq 3 + \log_S(1 + |\ell|) \quad \text{symbols.} \quad (48)$$

Let $\mathbf{x} = (x_n)_{n=1}^d$. We now study the result with 1) the deterministic quantizer, and 2) the probabilistic quantizer with $\mathbb{E}[\mathcal{Q}(x)] = x$.

Note that for the deterministic and probabilistic quantizers, we can express $\ell(x)$ as

$$|\ell(x)| \leq \lceil c_1 + c_2 \ln(1 + \omega/\eta|x|) \rceil,$$

for some $c_1 \leq 0$, $c_2 > 0$ (see (14) and (17) for a closed-form expression of c_1 and c_2). Invoking

(48) and $\bar{C}_{\text{comm}}(\mathbf{x}) = \sum_{n=1}^d \bar{C}_{\text{comm}}(\ell_n)$ yields

$$\begin{aligned} C(\mathbf{x}) &\leq 3d + \sum_{n=1}^d \log_S \left(1 + \lceil c_1 + c_2 \ln \left(1 + \frac{\omega|x_n|}{\eta} \right) \rceil \right) \\ &\stackrel{(a)}{\leq} 3d + d \log_S \left(2 + c_1 + c_2 \ln \left(1 + \frac{\omega\|\mathbf{x}\|_2}{\sqrt{d}\eta} \right) \right) \quad \text{symbols} \\ &= \log_2(S + 1) \left[3d + d \log_S \left(2 + c_1 + c_2 \ln \left(1 + \frac{\omega\|\mathbf{x}\|_2}{\sqrt{d}\eta} \right) \right) \right] \quad \text{bits,} \end{aligned} \quad (49)$$

where (a) follows from $\lceil x \rceil \leq x + 1$, Jensen's inequality and Cauchy–Schwarz inequality, in order. Invoking the expressions of c_1 and c_2 from (14) and (17), respectively, yield the result for the deterministic and probabilistic quantizers with odd N . Similar techniques can be used to find $\ell(x)$ and thus the result for quantizers with even N .

APPENDIX D

EXAMPLES OF (M)

In this section, we will show that (M) contains a gamut of distributed algorithms, corresponding to different choices of R , \mathcal{C}_i^s , and \mathcal{A}_i . Given (P), we will assume that each f_i is L -smooth and μ -strongly convex.

Every distributed algorithm on mesh networks we will describe below alternates one step of optimization with possibly multiple rounds of communications. In each communication round, every agent i combines linearly the signal received by its neighbors using weights $(w_{ij})_{j \in \mathcal{N}_i}$; let $\mathbf{W} = (w_{ij})_{i,j=1}^m$. Consistently with the undirected graph \mathcal{G} , we will tacitly assume that \mathbf{W}

is symmetric and doubly stochastic, i.e., $\mathbf{W} = \mathbf{W}^\top$ and $\mathbf{W}\mathbf{1} = \mathbf{1}$, with $w_{ij} > 0$ if $(j, i) \in \mathcal{E}$, and $w_{ij} = 0$ otherwise. We assume that the eigenvalues of \mathbf{W} are in $[\nu, 1]$, with $\nu > 0$.⁶ Note that this condition can be achieved by design: in fact, given a doubly stochastic weight matrix $\tilde{\mathbf{W}} = (\tilde{w}_{ij})_{i,j \in [m]}$, each agent i can set $w_{ii} = [(1+\nu) + (1-\nu)\tilde{w}_{ii}]/2$ and $w_{ij} = (1-\nu)\tilde{w}_{ij}/2, \forall j \neq i$ for a design parameter $\nu \in (0, 1]$. Note that, for any given \mathbf{z}^0 and \mathbf{z}^∞ with bounded entries, it holds $\|\mathbf{z}^0 - \mathbf{z}^\infty\|_2 = \mathcal{O}(\sqrt{md})$.

Finally, in the rest of this section, we will adopt the following notations: $\mathbf{x}^k = (\mathbf{x}_i^k)_{i=1}^m, \mathbf{y}^k = (\mathbf{y}_i^k)_{i=1}^m, \mathbf{w}^k = (\mathbf{w}_i^k)_{i=1}^m, \mathbf{x} = (\mathbf{x}_i)_{i=1}^m, \mathbf{y} = (\mathbf{y}_i)_{i=1}^m$ and $\mathbf{w} = (\mathbf{w}_i)_{i=1}^m, \hat{\mathbf{W}} = \mathbf{W} \otimes \mathbf{I}_d$, and \mathbf{G}^\dagger is the pseudo-inverse of matrix \mathbf{G} . Given $\mathbf{x}^k = (\mathbf{x}_i^k)_{i=1}^m$, we also define $\nabla f(\mathbf{x}^k) \triangleq (\nabla f_i(\mathbf{x}_i^k))_{i=1}^m$. For any function $g : \mathbb{R}^d \rightarrow \mathbb{R}$ and positive semi-definite matrix \mathbf{G} , define $\|\mathbf{x}\|_{\mathbf{G}} \triangleq \sqrt{\mathbf{x}^\top \mathbf{G} \mathbf{x}}$ and

$$\text{prox}_{\mathbf{G},g}(\mathbf{x}) \triangleq \arg \min_{\mathbf{z} \in \mathbb{R}^d} g(\mathbf{z}) + \frac{1}{2} \|\mathbf{z} - \mathbf{x}\|_{\mathbf{G}^{-1}}^2.$$

A. (Prox-)EXTRA [47]

The update of prox-EXTRA solving (P) reads

$$\begin{aligned} \mathbf{x}^k &= \text{prox}_{\gamma \mathbf{I}, r}(\mathbf{w}^k), \\ \mathbf{y}^{k+1} &= \mathbf{y}^k + (\mathbf{I} - \hat{\mathbf{W}}) \mathbf{w}^{k+1}, \\ \mathbf{w}^{k+1} &= \hat{\mathbf{W}} \mathbf{x}^k - \gamma \nabla f(\mathbf{x}^k) - \mathbf{y}^k, \end{aligned}$$

with $\mathbf{y}^0 = \mathbf{0}$ and $\mathbf{w}^0 \in \mathbb{R}^{md}$.

Prox-EXTRA can be cast as (M) with $R = 2$ rounds of communications with

$$\mathbf{z}^\top = [\mathbf{y}^\top, \mathbf{w}^\top],$$

$$\hat{\mathbf{c}}_i^{k,1} = \mathcal{C}_i^1(\mathbf{z}_i^k, \mathbf{0}) = \text{prox}_{\gamma \mathbf{I}, r}(\mathbf{w}_i^k), \quad (50)$$

$$\hat{\mathbf{c}}_i^{k,2} = \mathcal{C}_i^2(\mathbf{z}_i^k, \hat{\mathbf{c}}_{\mathcal{N}_i}^{k,1}) = \sum_{j \in \mathcal{N}_i} w_{ij} \hat{\mathbf{c}}_j^{k,1} - \gamma \nabla f_i(\hat{\mathbf{c}}_i^{k,1}) - \mathbf{y}_i^k, \quad (51)$$

$$\mathbf{z}_i^{k+1} = \mathcal{A}_i(\mathbf{z}_i^k, \hat{\mathbf{c}}_{\mathcal{N}_i}^{k,1}, \hat{\mathbf{c}}_{\mathcal{N}_i}^{k,2}) = \begin{bmatrix} \mathbf{y}_i^k + \hat{\mathbf{c}}_i^{k,2} - \sum_{j \in \mathcal{N}_i} w_{ij} \hat{\mathbf{c}}_j^{k,2} \\ \hat{\mathbf{c}}_i^{k,2} \end{bmatrix}. \quad (52)$$

We show next that the above instance of (M) satisfies Assumptions 1, 4, 5, and 11.

⁶This assumption is also required in [47] for prox-EXTRA, prox-NEXT, prox-DIGing, and prox-NIDS for achieving $\|\mathbf{z}^k - \mathbf{z}^\infty\| = \mathcal{O}(\sqrt{md}(\lambda)^k)$.

• **On Assumption 1:** Using [47] it is not difficult to check that, if $\gamma = \frac{2\rho_m(\mathbf{W})}{L+\mu\rho_m(\mathbf{W})}$, then prox-EXTRA satisfies Assumption 1, with some $\lambda < 1$ and the norm $\|\bullet\|$ defined as

$$\|\mathbf{z}\|^2 = \mathbf{w}^\top \hat{\mathbf{W}}^{-1} \mathbf{w} + \mathbf{y}^\top (\mathbf{I} - \hat{\mathbf{W}})^\dagger \mathbf{y}.$$

Note that $\|\mathbf{z}\|^2 \geq \|\mathbf{z}\|_2^2$, due to $\rho_i(\mathbf{W}) \in [\nu, 1]$, $i \in [m]$.

• **On Assumptions 4, 5, and 11:** Based on (50), (51) and (52), the mappings \mathcal{A} and \mathcal{C} read

$$\mathcal{A}(\mathbf{z}, \mathbf{c}^1, \mathbf{c}^2) = \begin{bmatrix} \mathbf{y} + (\mathbf{I} - \hat{\mathbf{W}}) \mathbf{c}^2 \\ \mathbf{c}^2 \end{bmatrix},$$

$$\mathcal{C}^1(\mathbf{z}, \mathbf{0}) = \text{prox}_{\gamma \mathbf{I}, r}(\mathbf{w}), \quad \text{and} \quad \mathcal{C}^2(\mathbf{z}, \mathbf{c}) = \hat{\mathbf{W}} \mathbf{c} - \gamma \nabla f(\mathbf{c}) - \mathbf{y},$$

respectively; and $\mathcal{Z} = \text{span}(\mathbf{I} - \hat{\mathbf{W}}) \times \mathbb{R}^{md}$, where we defined (with a slight abuse of notation)

$$\text{prox}_{\gamma \mathbf{I}, r}(\mathbf{w}) = (\text{prox}_{\gamma \mathbf{I}, r}(\mathbf{w}_i))_{i=1}^m.$$

We show that prox-EXTRA satisfies Assumption 11. Note that

$$\begin{aligned} \|\mathcal{A}(\mathbf{z}, \mathbf{c}^1, \mathbf{c}) - \mathcal{A}(\mathbf{z}, \mathbf{c}^1, \mathbf{c}')\|^2 &= \|\sqrt{\hat{\mathbf{W}}^{-1}}(\mathbf{c} - \mathbf{c}')\|_2^2 + \|\sqrt{\mathbf{I} - \hat{\mathbf{W}}}(\mathbf{c} - \mathbf{c}')\|_2^2 \\ &\leq (1 + \nu^{-1}) \|\mathbf{c} - \mathbf{c}'\|_2^2, \end{aligned}$$

and $\mathcal{A}(\mathbf{z}, \mathbf{c}^1, \mathbf{c}^2)$ is constant with respect to \mathbf{c}^1 , hence Assumption 4 holds with $L_A = \sqrt{1 + \nu^{-1}}$.

We next derive L_C and L_Z . Since the proximal mapping is non-expansive [57], it follows that

$$\begin{aligned} \|\mathcal{C}^1(\mathbf{z}, \mathbf{0}) - \mathcal{C}^1(\mathbf{z}', \mathbf{0})\|_2 &= \|\text{prox}_{\gamma \mathbf{I}, r}(\mathbf{w}) - \text{prox}_{\gamma \mathbf{I}, r}(\mathbf{w}')\|_2 \leq \|\mathbf{w} - \mathbf{w}'\|_2 \leq \|\mathbf{z} - \mathbf{z}'\|_2, \\ \|\mathcal{C}^2(\mathbf{z}, \mathbf{c}) - \mathcal{C}^2(\mathbf{z}', \mathbf{c}')\|_2 &= \|\hat{\mathbf{W}}(\mathbf{c} - \mathbf{c}') - \gamma(\nabla f(\mathbf{c}) - \nabla f(\mathbf{c}')) - (\mathbf{y} - \mathbf{y}')\|_2 \\ &\leq \|\mathbf{c} - \mathbf{c}'\|_2 + \gamma L \|\mathbf{c} - \mathbf{c}'\|_2 + \|\mathbf{z} - \mathbf{z}'\|_2, \end{aligned}$$

Assumption 5 holds with $L_C = 1 + \gamma L$ and $L_Z = 1$. Since $\gamma = \mathcal{O}(1/L)$, it follows that $L_C = \mathcal{O}(1)$. For the initial conditions, we have

$$\begin{aligned} \|\mathcal{C}^1(\mathbf{z}^0, \mathbf{0})\|_2 &= \|\text{prox}_{\gamma \mathbf{I}, r}(\mathbf{w}^0)\|_2 \stackrel{(a)}{\leq} \|\text{prox}_{\gamma \mathbf{I}, r}(\mathbf{w}^0) - \text{prox}_{\gamma \mathbf{I}, r}(\mathbf{w}^\infty)\|_2 + \|\text{prox}_{\gamma \mathbf{I}, r}(\mathbf{w}^\infty)\|_2 \\ &\stackrel{(b)}{\leq} \|\mathbf{w}^0 - \mathbf{w}^\infty\|_2 + \|\mathbf{w}^\infty\|_2 = \mathcal{O}(\sqrt{md}), \\ \|\mathcal{C}^2(\mathbf{z}^0, \mathbf{0})\|_2 &= \|\mathbf{y}^0\|_2 \leq \|\mathbf{y}^0 - \mathbf{y}^\infty\|_2 + \|\mathbf{y}^\infty\|_2 = \mathcal{O}(\sqrt{md}), \end{aligned}$$

where (a) follows from the triangle inequality; and (b) follows from the non-expansive property of the proximal mapping and \mathbf{w}^∞ is a fixed point of the proximal mapping [47].

Therefore, $L_A L_Z = \mathcal{O}(1)$, $L_C = \mathcal{O}(1)$, $\|\mathcal{C}^1(\mathbf{z}^0, \mathbf{0})\|_2 = \mathcal{O}(L_Z \sqrt{md})$ and $\|\mathcal{C}^2(\mathbf{z}^0, \mathbf{0})\|_2 = \mathcal{O}(L_Z \sqrt{md})$; hence Assumption 11 holds.

B. (Prox-)NEXT [47]

The update of prox-NEXT solving (P) reads

$$\begin{aligned}\mathbf{x}^k &= \text{prox}_{\gamma\mathbf{I},r}(\mathbf{w}^k), \\ \mathbf{y}^{k+1} &= \mathbf{y}^k + (\mathbf{I} - \hat{\mathbf{W}})^2 \mathbf{w}^{k+1}, \\ \mathbf{w}^{k+1} &= \hat{\mathbf{W}}^2 (\mathbf{x}^k - \gamma \nabla f(\mathbf{x}^k)) - \mathbf{y}^k,\end{aligned}$$

with $\mathbf{y}^0 = \mathbf{0}$ and $\mathbf{w}^0 \in \mathbb{R}^{md}$.

Prox-NEXT can be cast as (M) with $R = 4$ rounds of communications, using the following definitions:

$$\mathbf{z}^\top = [\mathbf{y}^\top, \mathbf{w}^\top],$$

$$\hat{\mathbf{c}}_i^{k,1} = \mathcal{C}_i^1(\mathbf{z}_i^k, \mathbf{0}) = \text{prox}_{\gamma\mathbf{I},r}(\mathbf{w}_i^k) - \gamma \nabla f_i(\text{prox}_{\gamma\mathbf{I},r}(\mathbf{w}_i^k)), \quad (53)$$

$$\hat{\mathbf{c}}_i^{k,2} = \mathcal{C}_i^2(\mathbf{z}_i^k, \hat{\mathbf{c}}_{\mathcal{N}_i}^{k,1}) = \sum_{j \in \mathcal{N}_i} w_{ij} \hat{\mathbf{c}}_j^{k,1}, \quad (54)$$

$$\hat{\mathbf{c}}_i^{k,3} = \mathcal{C}_i^3(\mathbf{z}_i^k, \hat{\mathbf{c}}_{\mathcal{N}_i}^{k,2}) = \sum_{j \in \mathcal{N}_i} w_{ij} \hat{\mathbf{c}}_j^{k,2} - \mathbf{y}_i^k, \quad (55)$$

$$\hat{\mathbf{c}}_i^{k,4} = \mathcal{C}_i^4(\mathbf{z}_i^k, \hat{\mathbf{c}}_{\mathcal{N}_i}^{k,3}) = \sum_{j \in \mathcal{N}_i} w_{ij} (\hat{\mathbf{c}}_i^{k,3} - \hat{\mathbf{c}}_j^{k,3}), \quad (56)$$

$$\mathbf{z}_i^{k+1} = \mathcal{A}_i(\mathbf{z}_i^k, \hat{\mathbf{c}}_{\mathcal{N}_i}^{k,1}, \hat{\mathbf{c}}_{\mathcal{N}_i}^{k,2}, \hat{\mathbf{c}}_{\mathcal{N}_i}^{k,3}, \hat{\mathbf{c}}_{\mathcal{N}_i}^{k,4}) = \begin{bmatrix} \mathbf{y}_i^k + \sum_{j \in \mathcal{N}_i} w_{ij} (\hat{\mathbf{c}}_i^{k,4} - \hat{\mathbf{c}}_j^{k,4}) \\ \hat{\mathbf{c}}_i^{k,3} \end{bmatrix}. \quad (57)$$

We show next that the above instance of (M) satisfies Assumptions 1, 4, 5, and 11.

- **On Assumption 1:** Using [47] it is not difficult to check that, if $\gamma = 2/(\mu + L)$, then prox-NEXT satisfies Assumption 1, with $\lambda < 1$ and the norm $\|\bullet\|$ defined as

$$\|\mathbf{z}\|^2 = \|\hat{\mathbf{W}}^{-2} \mathbf{w}\|_{\mathbf{I} - (\mathbf{I} - \hat{\mathbf{W}})^2}^2 + \mathbf{y} (\hat{\mathbf{W}}^{-2} ((\mathbf{I} - \hat{\mathbf{W}})^2)^\dagger \hat{\mathbf{W}}^{-2}) \mathbf{y}.$$

Again, note that $\|\mathbf{z}\|^2 \geq \|\mathbf{z}\|_2^2$.

- **On Assumptions 4, 5, and 11:** Based on (53)-(57), the mappings \mathcal{A} and \mathcal{C} read

$$\mathcal{A}(\mathbf{z}, \mathbf{c}^1, \mathbf{c}^2, \mathbf{c}^3, \mathbf{c}^4) = \begin{bmatrix} \mathbf{y} + (\mathbf{I} - \hat{\mathbf{W}}) \mathbf{c}^4 \\ \mathbf{c}^3 \end{bmatrix},$$

$$\mathcal{C}^1(\mathbf{z}, \mathbf{0}) = \text{prox}_{\gamma\mathbf{I},r}(\mathbf{w}) - \gamma \nabla f(\text{prox}_{\gamma\mathbf{I},r}(\mathbf{w})), \quad \mathcal{C}^2(\mathbf{z}, \mathbf{c}) = \hat{\mathbf{W}} \mathbf{c},$$

$$\mathcal{C}^3(\mathbf{z}, \mathbf{c}) = \hat{\mathbf{W}} \mathbf{c} - \mathbf{y}, \quad \text{and} \quad \mathcal{C}^4(\mathbf{z}, \mathbf{c}) = (\mathbf{I} - \hat{\mathbf{W}}) \mathbf{c},$$

respectively; and $\mathcal{Z} = \text{span}(\mathbf{I} - \hat{\mathbf{W}}) \times \mathbb{R}^{md}$.

We now show that prox-NEXT satisfies Assumption 11. Note that

$$\begin{aligned} & \|\mathcal{A}(\mathbf{z}, \mathbf{c}^1, \mathbf{c}^2, \mathbf{c}, \mathbf{c}^4) - \mathcal{A}(\mathbf{z}, \mathbf{c}^1, \mathbf{c}^2, \mathbf{c}', \mathbf{c}^4)\|^2 \\ &= (\mathbf{c} - \mathbf{c}')^\top \hat{\mathbf{W}}^{-4} [\mathbf{I} - (\mathbf{I} - \hat{\mathbf{W}})^2] (\mathbf{c} - \mathbf{c}') \leq \nu^{-2} (2\nu^{-1} - 1) \|\mathbf{c} - \mathbf{c}'\|_2^2 \end{aligned}$$

and

$$\|\mathcal{A}(\mathbf{z}, \mathbf{c}_1, \mathbf{c}_2, \mathbf{c}_3, \mathbf{c}) - \mathcal{A}(\mathbf{z}, \mathbf{c}_1, \mathbf{c}_2, \mathbf{c}_3, \mathbf{c}')\|^2 = \|\hat{\mathbf{W}}^{-2}(\mathbf{c} - \mathbf{c}')\|_2^2 \leq \nu^{-4} \|\mathbf{c} - \mathbf{c}'\|_2^2.$$

Moreover, $\mathcal{A}(\mathbf{z}, \mathbf{c}^1, \mathbf{c}^2, \mathbf{c}^3, \mathbf{c}^4)$ is constant with respect to $\mathbf{c}^1, \mathbf{c}^2$. Therefore, Assumption 4 holds with $L_A = \sqrt{2}\nu^{-2}$.

We next derive L_C and L_Z . Using the non-expansive property, it follows that

$$\begin{aligned} & \|\mathcal{C}^1(\mathbf{z}, \mathbf{0}) - \mathcal{C}^1(\mathbf{z}', \mathbf{0})\|_2 \\ &= \|(\text{prox}_{\gamma\mathbf{I},r}(\mathbf{w}) - \text{prox}_{\gamma\mathbf{I},r}(\mathbf{w}')) - \gamma(\nabla f(\text{prox}_{\gamma\mathbf{I},r}(\mathbf{w})) - \nabla f(\text{prox}_{\gamma\mathbf{I},r}(\mathbf{w}')))\|_2 \\ &\leq (1 + \gamma L) \|\text{prox}_{\gamma\mathbf{I},r}(\mathbf{w}) - \text{prox}_{\gamma\mathbf{I},r}(\mathbf{w}')\|_2 \leq (1 + \gamma L) \|\mathbf{w} - \mathbf{w}'\|_2 \leq (1 + \gamma L) \|\mathbf{z} - \mathbf{z}'\|_2, \\ & \|\mathcal{C}^2(\mathbf{c}, \mathbf{z}) - \mathcal{C}^2(\mathbf{c}', \mathbf{z}')\|_2 = \|\hat{\mathbf{W}}(\mathbf{c} - \mathbf{c}')\|_2 \leq \|\mathbf{c} - \mathbf{c}'\|_2, \\ & \|\mathcal{C}^3(\mathbf{c}, \mathbf{z}) - \mathcal{C}^3(\mathbf{c}', \mathbf{z}')\|_2 \leq \|\hat{\mathbf{W}}(\mathbf{c} - \mathbf{c}')\|_2 + \|\mathbf{y} - \mathbf{y}'\|_2 \leq \|\mathbf{c} - \mathbf{c}'\|_2 + \|\mathbf{z} - \mathbf{z}'\|_2, \\ & \|\mathcal{C}^4(\mathbf{c}, \mathbf{z}) - \mathcal{C}^4(\mathbf{c}', \mathbf{z}')\|_2 = \|(\mathbf{I} - \hat{\mathbf{W}})(\mathbf{c} - \mathbf{c}')\|_2 \leq \|\mathbf{c} - \mathbf{c}'\|_2, \end{aligned}$$

which implies that Assumption 5 holds with $L_C = 1$ and $L_Z = 1 + \gamma L$. Since $\gamma = \mathcal{O}(1/L)$, it follows that $L_Z = \mathcal{O}(1)$. For the initial conditions, we have $\|\mathcal{C}^1(\mathbf{z}^0, \mathbf{0})\|_2 \leq (1 + \gamma L)(\|\mathbf{w}^0 - \mathbf{w}^\infty\|_2 + \|\mathbf{w}^\infty\|_2) = \mathcal{O}(\sqrt{md})$ and $\|\mathcal{C}^3(\mathbf{z}^0, \mathbf{0})\|_2 \leq \|\mathbf{y}^0 - \mathbf{y}^\infty\|_2 + \|\mathbf{y}^\infty\|_2 = \mathcal{O}(\sqrt{md})$.

Therefore, $L_A L_Z = \mathcal{O}(1)$, $L_C = \mathcal{O}(1)$, $\|\mathcal{C}^1(\mathbf{z}^0, \mathbf{0})\|_2 = \mathcal{O}(L_Z \sqrt{md})$, $\|\mathcal{C}^2(\mathbf{z}^0, \mathbf{0})\|_2 = 0$, $\|\mathcal{C}^3(\mathbf{z}^0, \mathbf{0})\|_2 = \mathcal{O}(L_Z \sqrt{md})$, and $\|\mathcal{C}^4(\mathbf{z}^0, \mathbf{0})\|_2 = 0$; hence Assumption 11 holds.

C. (Prox-)DIGing [47]

The update of prox-DIGing solving (P), reads

$$\begin{aligned} \mathbf{x}^k &= \text{prox}_{\gamma\mathbf{I},r}(\mathbf{w}^k), \\ \mathbf{y}^{k+1} &= \mathbf{y}^k + (\mathbf{I} - \hat{\mathbf{W}})^2 \mathbf{w}^{k+1}, \\ \mathbf{w}^{k+1} &= \hat{\mathbf{W}}^2 \mathbf{x}^k - \gamma \nabla f(\mathbf{x}^k) - \mathbf{y}^k, \end{aligned}$$

with $\mathbf{y}^0 = \mathbf{0}$ and $\mathbf{w}^0 \in \mathbb{R}^{md}$.

Prox-DIGing can be cast as (M) with $R = 4$ rounds of communications, using the following definitions:

$$\mathbf{z}^\top = [\mathbf{y}^\top, \mathbf{w}^\top],$$

$$\hat{\mathbf{c}}_i^{k,1} = \mathcal{C}_i^1(\mathbf{z}_i^k, \mathbf{0}) = \text{prox}_{\gamma\mathbf{I},r}(\mathbf{w}_i^k), \quad (58)$$

$$\hat{\mathbf{c}}_i^{k,2} = \mathcal{C}_i^2(\mathbf{z}_i^k, \hat{\mathbf{c}}_{\mathcal{N}_i}^{k,1}) = \sum_{j \in \mathcal{N}_i} w_{ij} \hat{\mathbf{c}}_j^{k,1}, \quad (59)$$

$$\hat{\mathbf{c}}_i^{k,3} = \mathcal{C}_i^3(\mathbf{z}_i^k, \hat{\mathbf{c}}_{\mathcal{N}_i}^{k,2}) = \sum_{j \in \mathcal{N}_i} w_{ij} \hat{\mathbf{c}}_j^{k,2} - \gamma \nabla f_i(\text{prox}_{\gamma\mathbf{I},r}(\mathbf{w}_i^k)) - \mathbf{y}_i^k, \quad (60)$$

$$\hat{\mathbf{c}}_i^{k,4} = \mathcal{C}_i^4(\mathbf{z}_i^k, \hat{\mathbf{c}}_{\mathcal{N}_i}^{k,3}) = \sum_{j \in \mathcal{N}_i} w_{ij} (\hat{\mathbf{c}}_j^{k,3} - \hat{\mathbf{c}}_i^{k,3}), \quad (61)$$

$$\mathbf{z}_i^{k+1} = \mathcal{A}_i(\mathbf{z}_i^k, \hat{\mathbf{c}}_{\mathcal{N}_i}^{k,1}, \hat{\mathbf{c}}_{\mathcal{N}_i}^{k,2}, \hat{\mathbf{c}}_{\mathcal{N}_i}^{k,3}, \hat{\mathbf{c}}_{\mathcal{N}_i}^{k,4}) = \begin{bmatrix} \mathbf{y}_i^k + \sum_{j \in \mathcal{N}_i} w_{ij} (\hat{\mathbf{c}}_i^{k,4} - \hat{\mathbf{c}}_j^{k,4}) \\ \hat{\mathbf{c}}_i^{k,3} \end{bmatrix}. \quad (62)$$

We show next that the above instance of (M) satisfies Assumptions 1, 4, 5, and 11.

• **On Assumption 1:** Using [47] it is not difficult to check that, if $\gamma = \frac{2\rho_1(\mathbf{W})}{L + \mu\rho_1(\mathbf{W})}$, then prox-DIGing satisfies Assumption 1, with $\lambda < 1$ and the norm $\|\bullet\|$ defined as

$$\|\mathbf{z}\|^2 = \frac{1}{2\nu - \nu^2} \left(\|\mathbf{w}\|_{\mathbf{I} - (\mathbf{I} - \hat{\mathbf{W}})^2}^2 + \mathbf{y}^\top ((\mathbf{I} - \hat{\mathbf{W}})^2)^\dagger \mathbf{y} \right).$$

Note that $\|\mathbf{z}\|^2 \geq \|\mathbf{z}\|_2^2$.

• **On Assumptions 4, 5, and 11:** Based on (58)-(62), the mappings \mathcal{A} and \mathcal{C} read

$$\mathcal{A}(\mathbf{z}, \mathbf{c}^1, \mathbf{c}^2, \mathbf{c}^3, \mathbf{c}^4) = \begin{bmatrix} \mathbf{y} + (\mathbf{I} - \hat{\mathbf{W}})\mathbf{c}^4 \\ \mathbf{c}^3 \end{bmatrix},$$

$$\mathcal{C}^1(\mathbf{z}, \mathbf{0}) = \text{prox}_{\gamma\mathbf{I},r}(\mathbf{w}), \quad \mathcal{C}^2(\mathbf{z}, \mathbf{c}) = \hat{\mathbf{W}}\mathbf{c},$$

$$\mathcal{C}^3(\mathbf{z}, \mathbf{c}) = \hat{\mathbf{W}}\mathbf{c} - \gamma \nabla f(\text{prox}_{\gamma\mathbf{I},r}(\mathbf{w})) - \mathbf{y}, \quad \text{and} \quad \mathcal{C}^4(\mathbf{z}, \mathbf{c}) = (\mathbf{I} - \hat{\mathbf{W}})\mathbf{c},$$

respectively; and $\mathcal{Z} = \text{span}(\mathbf{I} - \hat{\mathbf{W}}) \times \mathbb{R}^{md}$. We now show that prox-DIGing satisfies Assumption 11. Note that

$$\begin{aligned} \|\mathcal{A}(\mathbf{z}, \mathbf{c}_1, \mathbf{c}_2, \mathbf{c}, \mathbf{c}^4) - \mathcal{A}(\mathbf{z}, \mathbf{c}_1, \mathbf{c}_2, \mathbf{c}', \mathbf{c}^4)\|^2 &= \frac{1}{2\nu - \nu^2} (\mathbf{c} - \mathbf{c}')^\top [\mathbf{I} - (\mathbf{I} - \hat{\mathbf{W}})^2] (\mathbf{c} - \mathbf{c}') \\ &\leq \frac{1}{2\nu - \nu^2} \|\mathbf{c} - \mathbf{c}'\|_2^2, \end{aligned}$$

and

$$\|\mathcal{A}(\mathbf{z}, \mathbf{c}_1, \mathbf{c}_2, \mathbf{c}_3, \mathbf{c}) - \mathcal{A}(\mathbf{z}, \mathbf{c}_1, \mathbf{c}_2, \mathbf{c}_3, \mathbf{c}')\|^2 = \frac{1}{2\nu - \nu^2} \|\mathbf{c} - \mathbf{c}'\|_2^2.$$

Moreover, $\mathcal{A}(\mathbf{z}, \mathbf{c}^1, \mathbf{c}^2, \mathbf{c}^3, \mathbf{c}^4)$ is constant with respect to $\mathbf{c}^1, \mathbf{c}^2$. Therefore, Assumption 4 holds with $L_A = \sqrt{1/(2\nu - \nu^2)}$.

We next derive L_C and L_Z . We have

$$\begin{aligned}\|\mathcal{C}^1(\mathbf{z}, \mathbf{0}) - \mathcal{C}^1(\mathbf{z}', \mathbf{0})\|_2 &\leq (1 + \gamma L)\|\mathbf{z} - \mathbf{z}'\|_2, \\ \|\mathcal{C}^2(\mathbf{z}, \mathbf{c}) - \mathcal{C}^2(\mathbf{z}', \mathbf{c}')\|_2 &= \|\hat{\mathbf{W}}(\mathbf{c} - \mathbf{c}')\|_2 \leq \|\mathbf{c} - \mathbf{c}'\|_2, \\ \|\mathcal{C}^3(\mathbf{z}, \mathbf{c}) - \mathcal{C}^3(\mathbf{z}', \mathbf{c}')\|_2 &\leq \|\mathbf{c} - \mathbf{c}'\|_2 + (1 + \gamma L)\|\mathbf{z} - \mathbf{z}'\|_2, \\ \|\mathcal{C}^4(\mathbf{z}, \mathbf{c}) - \mathcal{C}^4(\mathbf{z}', \mathbf{c}')\|_2 &= \|(\mathbf{I} - \hat{\mathbf{W}})\mathbf{c} - \mathbf{c}'\|_2 \leq \|\mathbf{c} - \mathbf{c}'\|_2,\end{aligned}$$

which implies that Assumption 5 holds with $L_C = 1$ and $L_Z = 1 + \gamma L$. Since $\gamma = \mathcal{O}(1/L)$, it follows that $L_Z = \mathcal{O}(1)$. For the initial conditions, we have $\|\mathcal{C}^1(\mathbf{z}^0, \mathbf{0})\|_2 \leq \|\mathbf{w}^0 - \mathbf{w}^\infty\|_2 + \|\mathbf{w}^\infty\|_2 = \mathcal{O}(\sqrt{md})$ and $\|\mathcal{C}^3(\mathbf{z}^0, \mathbf{0})\|_2 \leq \gamma L(\|\mathbf{w}^0 - \mathbf{w}^\infty\|_2 + \|\mathbf{w}^\infty\|_2) + \|\mathbf{y}^0 - \mathbf{y}^\infty\|_2 + \|\mathbf{y}^\infty\|_2 = \mathcal{O}(\sqrt{md})$.

Therefore, $L_A L_Z = \mathcal{O}(1)$, $L_C = \mathcal{O}(1)$, $\|\mathcal{C}^1(\mathbf{z}^0, \mathbf{0})\|_2 = \mathcal{O}(L_Z \sqrt{md})$, $\|\mathcal{C}^2(\mathbf{z}^0, \mathbf{0})\|_2 = 0$, $\|\mathcal{C}^3(\mathbf{z}^0, \mathbf{0})\|_2 = \mathcal{O}(L_Z \sqrt{md})$, and $\|\mathcal{C}^4(\mathbf{z}^0, \mathbf{0})\|_2 = 0$; hence Assumption 11 holds.

D. (Prox-)NIDS [47]

The update of prox-NIDS solving (P), reads

$$\begin{aligned}\mathbf{x}^k &= \text{prox}_{\gamma \mathbf{I}, r}(\mathbf{w}^k), \\ \mathbf{y}^{k+1} &= \mathbf{y}^k + (\mathbf{I} - \hat{\mathbf{W}})\mathbf{w}^{k+1}, \\ \mathbf{w}^{k+1} &= \hat{\mathbf{W}}(\mathbf{x}^k - \gamma \nabla f(\mathbf{x}^k)) - \mathbf{y}^k,\end{aligned}$$

with $\mathbf{y}^0 = \mathbf{0}$ and $\mathbf{w}^0 \in \mathbb{R}^{md}$.

Prox-NIDS can be cast as (M) with $R = 2$ rounds of communications, using the following:

$$\mathbf{z}^\top = [\mathbf{y}^\top, \mathbf{w}^\top]$$

$$\mathcal{C}_i^1(\mathbf{z}_i^k, \mathbf{0}) = \text{prox}_{\gamma \mathbf{I}, r}(\mathbf{w}_i^k) - \gamma \nabla f_i(\text{prox}_{\gamma \mathbf{I}, r}(\mathbf{w}_i^k)) \quad (63)$$

$$\mathcal{C}_i^2(\mathbf{z}_i^k, \hat{\mathbf{c}}_{\mathcal{N}_i}^{k,1}) = \sum_{j \in \mathcal{N}_i} w_{ij} \hat{\mathbf{c}}_j^{k,1} - \mathbf{y}_i^k, \quad (64)$$

$$\mathbf{z}_i^{k+1} = \mathcal{A}_i(\mathbf{z}_i^k, \hat{\mathbf{c}}_{\mathcal{N}_i}^{k,1}, \hat{\mathbf{c}}_{\mathcal{N}_i}^{k,2}) = \begin{bmatrix} \mathbf{y}_i^k - \sum_{j \in \mathcal{N}_i} w_{ij} (\hat{\mathbf{c}}_j^{k,2} - \hat{\mathbf{c}}_i^{k,2}) \\ \hat{\mathbf{c}}_i^{k,2} \end{bmatrix}. \quad (65)$$

We show next that the above instance of (M) satisfies Assumptions 1, 4, 5, and 11.

• **On Assumption 1:** Using [47] it is not difficult to check that, if $\gamma = 2/(\mu + L)$, then prox-NIDS satisfies Assumption 1, with $\lambda < 1$ and the norm $\|\bullet\|$ defined as

$$\|\mathbf{z}\|^2 = \mathbf{w}^\top \hat{\mathbf{W}}^{-1} \mathbf{w} + \mathbf{y}^\top \hat{\mathbf{W}}^{-1} (\mathbf{I} - \hat{\mathbf{W}})^\dagger \hat{\mathbf{W}}^{-1} \mathbf{y}.$$

Note that $\|\mathbf{z}\|^2 \geq \|\mathbf{z}\|_2^2$.

• **On Assumptions 4, 5, and 11:** Based on (63), (64), and (65), the mappings \mathcal{A} and \mathcal{C} read

$$\mathcal{A}(\mathbf{z}, \mathbf{c}^1, \mathbf{c}^2) = \begin{bmatrix} \mathbf{y} + (\mathbf{I} - \hat{\mathbf{W}}) \mathbf{c}^2 \\ \mathbf{c}^2 \end{bmatrix},$$

$$\mathcal{C}^1(\mathbf{z}, \mathbf{0}) = \text{prox}_{\gamma \mathbf{I}, r}(\mathbf{w}) - \gamma \nabla f(\text{prox}_{\gamma \mathbf{I}, r}(\mathbf{w})), \quad \text{and} \quad \mathcal{C}^2(\mathbf{z}, \mathbf{c}) = \hat{\mathbf{W}} \mathbf{c} - \mathbf{y},$$

respectively; and $\mathcal{Z} = \text{span}(\mathbf{I} - \hat{\mathbf{W}}) \times \mathbb{R}^{md}$. We now show that prox-NIDS satisfies Assumption 11. Note that

$$\|\mathcal{A}(\mathbf{z}, \mathbf{c}_1, \mathbf{c}) - \mathcal{A}(\mathbf{z}, \mathbf{c}_1, \mathbf{c}')\|^2 = \|\sqrt{\mathbf{I} - \hat{\mathbf{W}} \hat{\mathbf{W}}^{-1}} (\mathbf{c} - \mathbf{c}')\|_2^2 \leq (\nu^{-2} - \nu^{-1}) \|\mathbf{c} - \mathbf{c}'\|_2^2,$$

and $\mathcal{A}(\mathbf{z}, \mathbf{c}^1, \mathbf{c}^2)$ is constant with respect to \mathbf{c}^1 . It follows that Assumption 4 holds with $L_A = \sqrt{\nu^{-2} - \nu^{-1}}$.

We next derive L_C and L_Z . Using the non-expansive property of the proximal mapping, it holds

$$\begin{aligned} & \|\mathcal{C}^1(\mathbf{z}, \mathbf{0}) - \mathcal{C}^1(\mathbf{z}', \mathbf{0})\|_2 \\ &= \|(\text{prox}_{\gamma \mathbf{I}, r}(\mathbf{w}) - \text{prox}_{\gamma \mathbf{I}, r}(\mathbf{w}')) - \gamma(\nabla f(\text{prox}_{\gamma \mathbf{I}, r}(\mathbf{w})) - \nabla f(\text{prox}_{\gamma \mathbf{I}, r}(\mathbf{w}')))\|_2 \\ &\leq (1 + \gamma L) \|\text{prox}_{\gamma \mathbf{I}, r}(\mathbf{w}) - \text{prox}_{\gamma \mathbf{I}, r}(\mathbf{w}')\|_2 \leq (1 + \gamma L) \|\mathbf{w} - \mathbf{w}'\|_2 \leq (1 + \gamma L) \|\mathbf{z} - \mathbf{z}'\|_2, \\ & \|\mathcal{C}^2(\mathbf{z}, \mathbf{c}) - \mathcal{C}^2(\mathbf{z}', \mathbf{c}')\|_2 = \|\hat{\mathbf{W}}(\mathbf{c} - \mathbf{c}')\|_2 + \|\mathbf{z} - \mathbf{z}'\|_2 \leq \|\mathbf{c} - \mathbf{c}'\|_2 + \|\mathbf{z} - \mathbf{z}'\|_2, \end{aligned}$$

which implies that Assumption 5 holds with $L_C = 1$ and $L_Z = 1 + \gamma L$. Since $\gamma = \mathcal{O}(1/L)$, it follows that $L_Z = \mathcal{O}(1)$. For the initial conditions, we have $\|\mathcal{C}^1(\mathbf{z}^0, \mathbf{0})\|_2 \leq (1 + \gamma L) (\|\mathbf{w}^0 - \mathbf{w}^\infty\|_2 + \|\mathbf{w}^\infty\|_2) = \mathcal{O}(\sqrt{md})$ and $\|\mathcal{C}^2(\mathbf{z}^0, \mathbf{0})\|_2 \leq \|\mathbf{y}^0 - \mathbf{y}^\infty\|_2 + \|\mathbf{y}^\infty\|_2 = \mathcal{O}(\sqrt{md})$.

Therefore, $L_A L_Z = \mathcal{O}(1)$, $L_C = \mathcal{O}(1)$, $\|\mathcal{C}^1(\mathbf{z}^0, \mathbf{0})\|_2 = \mathcal{O}(L_Z \sqrt{md})$, and $\|\mathcal{C}^2(\mathbf{z}^0, \mathbf{0})\|_2 = \mathcal{O}(L_Z \sqrt{md})$; hence Assumption 11 holds.

E. GD over star networks [58]

Consider Problem (P) with $r = 0$ over a master/workers system. The GD update

$$\mathbf{x}^{k+1} = \mathbf{x}^k - \frac{\gamma}{m} \sum_{i=1}^m \nabla f_i(\mathbf{x}^k), \quad (66)$$

with $\mathbf{x}^0 \in \mathbb{R}^d$, is implemented at the master node as follows: at iteration k , the server broadcasts \mathbf{x}^k to the m agents; each agent i then computes its own gradient $\nabla f_i(\mathbf{x}^k)$ and sends it back to the master; upon collecting all local gradients, the server updates the variable \mathbf{x}^{k+1} according to (66).

The GD (66) can be cast as (M) with $R = 1$ round of communications, using the following:

$$\begin{aligned} \mathbf{z} &= \mathbf{1}_m \otimes \mathbf{x}, \\ \hat{\mathbf{c}}_i^{k,1} &= \mathcal{C}_i^1(\mathbf{z}_i^k, \mathbf{0}) = \nabla f_i(\mathbf{x}_i^k), \end{aligned} \quad (67)$$

$$\mathbf{z}^{k+1} = \mathcal{A}(\mathbf{z}^k, \hat{\mathbf{c}}_{[m]}^{k,1}) = \mathbf{x}^k - \frac{\gamma}{m} \sum_{i=1}^m \mathbf{1}_m \otimes \hat{\mathbf{c}}_i^{k,1}. \quad (68)$$

We show next that the above instance of (M) satisfies Assumptions 1, 4, 5, and 11.

• **On Assumption 1:** Using [58] it is not difficult to check that, if $\gamma = 2/(\mu + L)$, then GD over star networks satisfies Assumption 1, with $\lambda < 1$ and the norm $\|\bullet\|$ defined as

$$\|\mathbf{z}\| = \|\mathbf{x}\|_2.$$

Note that $\|\mathbf{z}\| \geq \|\mathbf{z}\|_2$.

• **On Assumptions 4, 5, and 11:** Based on (67) and (68), the mappings \mathcal{A} and \mathcal{C} read

$$\mathcal{A}(\mathbf{z}, \mathbf{c}^1) = \mathbf{z} - \frac{\gamma}{m} \sum_{i=1}^m \mathbf{1}_m \otimes \mathbf{c}_i, \quad \mathcal{C}^1(\mathbf{z}, \mathbf{0}) = \gamma \nabla f(\mathbf{z}),$$

respectively; and $\mathcal{Z} = \{\mathbf{1}_m \otimes \mathbf{x} : \mathbf{x} \in \mathbb{R}^d\}$.

We now show that GD over star networks satisfies Assumption 11. Since

$$\mathcal{A}(\mathbf{z}, \mathbf{c}) - \mathcal{A}(\mathbf{z}, \mathbf{c}') = -\frac{1}{m} \sum_{i=1}^m \mathbf{1}_m \otimes (\mathbf{c}_i - \mathbf{c}'_i),$$

we have

$$\|\mathcal{A}(\mathbf{z}, \mathbf{c}) - \mathcal{A}(\mathbf{z}, \mathbf{c}')\|^2 = \frac{1}{m} \left\| \sum_{i=1}^m \mathbf{c}_i - \mathbf{c}'_i \right\|_2^2 \leq \|\mathbf{c} - \mathbf{c}'\|_2^2.$$

Hence, Assumption 4 holds with $L_A = 1$.

We now derive L_C and L_Z . Note that

$$\|\mathcal{C}^1(\mathbf{z}, \mathbf{0}) - \mathcal{C}^1(\mathbf{z}', \mathbf{0})\|_2^2 \leq \gamma^2 L^2 \|\mathbf{z} - \mathbf{z}'\|_2^2,$$

which implies that Assumption 5 holds with $L_C = 0$ and $L_Z = \gamma L$. Since $\gamma = \mathcal{O}(1/L)$, it follows that $L_A L_Z = \mathcal{O}(1)$ and $\|\mathcal{C}^1(\mathbf{z}^0, \mathbf{0})\|_2 \leq \gamma L \|\mathbf{x} - \tilde{\mathbf{x}}^*\|_2 = \mathcal{O}(\sqrt{md})$, where $\tilde{\mathbf{x}}^* = (\tilde{\mathbf{x}}_i^*)_{i=1}^m$ with $\tilde{\mathbf{x}}_i^* = \arg \min_{\mathbf{x}_i} f_i(\mathbf{x}_i)$.

Therefore, $L_A L_Z = \mathcal{O}(1)$, $L_C = \mathcal{O}(1)$, $\|\mathcal{C}^1(\mathbf{z}^0, \mathbf{0})\|_2 = \mathcal{O}(L_Z \sqrt{md})$; hence Assumption 11 holds.

F. Primal-dual algorithm [12], [42]

Let $\mathbf{L} = (l_{ij})_{i,j=1}^m$ be the Laplacian matrix associated with the 0-1 adjacency matrix of \mathcal{G} , i.e., $l_{ii} = |\mathcal{N}_i \setminus \{i\}|$, $i \in [m]$; and $l_{ij} = -\mathbb{1}\{(i,j) \in \mathcal{E}, i \neq j \in [m]\}$; and $\hat{\mathbf{L}} = \mathbf{L} \otimes \mathbf{I}_d$.

The primal-dual algorithm solving (P), with $r = 0$, reads [12], [42]

$$\begin{aligned} \mathbf{y}_i^{k+1} &= \mathbf{y}_i^k + \gamma \sum_{j \in \mathcal{N}_i} l_{ij} \mathbf{x}_j^k, \\ \mathbf{x}_i^{k+1} &= \arg \min_{\mathbf{x}_i} f_i(\mathbf{x}_i) + \mathbf{x}_i^\top \mathbf{y}_i^{k+1}, \end{aligned}$$

with $\mathbf{y}_i^0 = \mathbf{0}$ and $\mathbf{x}_i^0 = \arg \min_{\mathbf{x}_i} f_i(\mathbf{x}_i)$.

The primal-dual algorithm can be cast in the form (M), with $R = 1$ round of communications, using the following:

$$\mathbf{z} = \mathbf{y}$$

$$\mathcal{C}_i^1(\mathbf{z}_i^k, \mathbf{0}) = \arg \min_{\mathbf{c}_i} f_i(\mathbf{c}_i) + \mathbf{c}_i^\top \mathbf{y}_i^k, \quad (69)$$

$$\mathbf{z}_i^{k+1} = \mathcal{A}_i(\mathbf{z}_i^k, \hat{\mathbf{c}}_{\mathcal{N}_i}^{k,1}) = \mathbf{y}_i^k + \gamma \sum_{j \in \mathcal{N}_i} l_{ij} \hat{\mathbf{c}}_j^{k,1}. \quad (70)$$

We show next that the above instance of (M) satisfies Assumptions 1, 4, 5, and 11.

• **On Assumption 1:** Define $\mathbf{M} = \sqrt{\Sigma} \mathbf{Q}$, where $\hat{\mathbf{L}} = \mathbf{Q}^\top \Sigma \mathbf{Q}$ is its eigenvalue decomposition, with Σ being diagonal with elements sorted in descending order; and let $\bar{\mathbf{M}}$ be the matrix containing the non-zero rows of \mathbf{M} . Using [12] it is not difficult to check that, if $\gamma = \frac{2L\mu}{\mu\rho_2(\mathbf{L}) + L\rho_m(\mathbf{L})}$, the primal-dual algorithm satisfies Assumption 1, with $\lambda < 1$ and the norm $\|\bullet\|$ defined as

$$\|\mathbf{z}\| = \sqrt{\rho_2(\mathbf{L})} \left\| (\bar{\mathbf{M}} \bar{\mathbf{M}}^\top)^{-1} \bar{\mathbf{M}} \mathbf{z} \right\|_2.$$

Note that $\|\mathbf{z}\| \geq \|\mathbf{z}\|_2$.

• **On Assumptions 4, 5, and 11:** Based on (69) and (70), the mappings \mathcal{A} and \mathcal{C} read

$$\mathcal{A}(\mathbf{z}, \mathbf{c}^1) = \mathbf{z} + \gamma \hat{\mathbf{L}} \mathbf{c}^1 \quad \text{and} \quad \mathcal{C}^1(\mathbf{z}, \mathbf{0}) = \begin{bmatrix} \arg \min_{\mathbf{c}} f_1(\mathbf{c}) + \mathbf{c}^\top \mathbf{z}_1 \\ \vdots \\ \arg \min_{\mathbf{c}} f_m(\mathbf{c}) + \mathbf{c}^\top \mathbf{z}_m \end{bmatrix},$$

respectively; and $\mathcal{Z} = \text{span}(\mathbf{L})$. We now show that the primal-dual algorithm satisfies Assumption 11. Note that

$$\mathcal{A}(\mathbf{z}, \mathbf{c}) - \mathcal{A}(\mathbf{z}, \mathbf{c}') = \gamma \hat{\mathbf{L}} (\mathbf{c} - \mathbf{c}').$$

It follows that

$$\begin{aligned} \|\mathcal{A}(\mathbf{z}, \mathbf{c}) - \mathcal{A}(\mathbf{z}, \mathbf{c}')\|^2 &= \gamma^2 \rho_2(\mathbf{L}) \left\| (\bar{\mathbf{M}}\bar{\mathbf{M}}^\top)^{-1} \bar{\mathbf{M}}\hat{\mathbf{L}}(\mathbf{c} - \mathbf{c}') \right\|_2^2 \\ &\leq \gamma^2 \rho_2(\mathbf{L}) \rho_m(\mathbf{L}) \|\mathbf{c} - \mathbf{c}'\|_2^2, \end{aligned}$$

which implies that Assumption 4 holds with $L_A = \gamma \sqrt{\rho_2(\mathbf{L}) \rho_m(\mathbf{L})}$. Using the expression of γ , it follows that $L_A = \mathcal{O}(\mu)$. Hence, for all the objective functions of (P) such that $\mu = \mathcal{O}(1)$, we also have $L_A = \mathcal{O}(1)$. For instance, this is the typical case of several machine learning problems where a regularization $\mu/2\|\mathbf{x}\|^2$ is enforced on the objective function to make it strongly convex, with $\mu = \mathcal{O}(1)$.

We now derive L_C and L_Z . Since

$$\|\mathcal{C}^1(\mathbf{z}, \mathbf{0}) - \mathcal{C}^1(\mathbf{z}', \mathbf{0})\|_2 = \|\mathbf{z} - \mathbf{z}'\|_2,$$

Assumption 5 holds with $L_C = 0$ and $L_Z = 1$. For the initial conditions, since $\mathbf{z}^0 = \mathbf{0}$ we have $\|\mathcal{C}^1(\mathbf{z}^0, \mathbf{0})\|_2 = \|\tilde{\mathbf{x}}^*\|_2 = \mathcal{O}(\sqrt{md})$, where $\tilde{\mathbf{x}}_i^* = (\tilde{\mathbf{x}}_i^*)_{i=1}^m$ with $\tilde{\mathbf{x}}_i^* \triangleq \arg \min_{\mathbf{x}_i} f_i(\mathbf{x}_i)$.

Therefore, $L_A L_Z = \mathcal{O}(1)$, $L_C = \mathcal{O}(1)$, and $\|\mathcal{C}^1(\mathbf{z}^0, \mathbf{0})\|_2 = \mathcal{O}(L_Z \sqrt{md})$, when $\mu = \mathcal{O}(1)$; hence Assumption 11 holds.

REFERENCES

- [1] D. K. Molzahn, F. Dörfler, H. Sandberg, S. H. Low, S. Chakrabarti, R. Baldick, and J. Lavaei, "A survey of distributed optimization and control algorithms for electric power systems," *IEEE Trans. Smart Grid*, vol. 8, no. 6, pp. 2941–2962, Nov. 2017.
- [2] A. Nedić, J.-S. Pang, G. Scutari, and Y. Sun, *Multi-agent Optimization*, 1st ed. Springer, Cham, 2018.
- [3] T. Yang, X. Yi, J. Wu, Y. Yuan, D. Wu, Z. Meng, Y. Hong, H. Wang, Z. Lin, and K. H. Johansson, "A survey of distributed optimization," *Annual Reviews in Control*, vol. 47, pp. 278–305, May 2019.
- [4] R. Bekkerman, M. Bilenko, and J. Langford, *Scaling up Machine Learning: Parallel and Distributed Approaches*. Cambridge University Press, 2011.
- [5] X. Lian, C. Zhang, H. Zhang, C.-J. Hsieh, W. Zhang, and J. Liu., "Can decentralized algorithms outperform centralized algorithms? A case study for decentralized parallel stochastic gradient descent," in *Proc. 31st NeurIPS*, Dec. 2017.
- [6] H. Tang, S. Gan, C. Zhang, T. Zhang, and J. Liu, "Communication compression for decentralized training," in *Proc. 32nd NeurIPS*, Dec. 2018.
- [7] H. Taheri, A. Mokhtari, H. Hassani, and R. Pedarsani, "Quantized decentralized stochastic learning over directed graphs," in *Proc. 37th ICML*, Jul. 2020.
- [8] A. Beznosikov, S. Horváth, P. Richtárik, and M. Safaryan, "On biased compression for distributed learning," *arXiv:2002.12410v1*, Feb. 2020.
- [9] D. Kovalev, A. Koloskova, M. Jaggi, P. Richtárik, and S. U. Stich, "A linearly convergent algorithm for decentralized optimization: Sending less bits for free!" in *Proc. 24th AISTATS*, Apr. 2021.

- [10] Y. Liao, Z. Li, K. Huang, and S. Pu, “Compressed gradient tracking methods for decentralized optimization with linear convergence,” *arXiv:2103.13748v3*, Jun. 2021.
- [11] X. Liu, Y. Li, R. Wang, J. Tang, and M. Yan, “Linear convergent decentralized optimization with compression,” in *Proc. 9th ICLR*, May 2021.
- [12] S. Magnússon, H. Shokri-Ghadikolaei, and N. Li, “On maintaining linear convergence of distributed learning and optimization under limited communication,” *IEEE Trans. Signal Process.*, vol. 68, pp. 6101–6116, Oct. 2020.
- [13] Y. Kajiyama, N. Hayashi, and S. Takai, “Linear convergence of consensus-based quantized optimization for smooth and strongly convex cost functions,” *IEEE Trans. Autom. Control (Early Access)*, pp. 1–1, 2020.
- [14] C.-S. Lee, N. Michelusi, and G. Scutari, “Finite rate quantized distributed optimization with geometric convergence,” in *Proc. 52nd ACSSC*, Oct. 2018, pp. 1876–1880.
- [15] P. Di Lorenzo and G. Scutari, “Next: In-network nonconvex optimization,” *IEEE Trans. Signal Inf. Process. Netw.*, vol. 2, no. 2, pp. 120–136, Jun. 2016.
- [16] Y. Sun, A. Daneshmand, and G. Scutari, “Distributed optimization based on gradient-tracking revisited: Enhancing convergence rate via surrogation,” *arXiv:1905.02637v2*, May 2019.
- [17] G. Scutari and Y. Sun, “Distributed nonconvex constrained optimization over time-varying digraphs,” *Math. Program.*, vol. 176, p. 497–544, Feb. 2019.
- [18] A. Kashyap, T. Basar, and R. Srikant, “Quantized consensus,” *Automatica*, vol. 43, no. 7, pp. 1192–1203, May 2007.
- [19] T. C. Aysal, M. J. Coates, and M. G. Rabbat, “Distributed average consensus with dithered quantization,” *IEEE Trans. Signal Process.*, vol. 53, no. 10, pp. 4905–4918, Oct. 2008.
- [20] A. Nedić, A. Olshevsky, A. Ozdaglar, and J. N. Tsitsiklis, “On distributed averaging algorithms and quantization effects,” *IEEE Trans. Autom. Control*, vol. 54, no. 11, pp. 2506–2517, Nov. 2009.
- [21] S. Kar and J. M. F. Moura, “Distributed consensus algorithms in sensor networks: Quantized data and random link failures,” *IEEE Trans. Signal Process.*, vol. 58, no. 3, pp. 1383–1400, Mar. 2010.
- [22] T. Li, M. Fu, L. Xie, and J.-F. Zhang, “Distributed consensus with limited communication data rate,” *IEEE Trans. Autom. Control*, vol. 56, no. 2, pp. 279–292, Feb. 2011.
- [23] R. Rajagopal and M. J. Wainwright, “Network-based consensus averaging with general noisy channels,” *IEEE Trans. Signal Process.*, vol. 59, no. 1, pp. 373–385, Jan. 2011.
- [24] J. Lavaei and R. M. Murray, “Quantized consensus by means of gossip algorithm,” *IEEE Trans. Autom. Control*, vol. 57, no. 1, pp. 19–32, Jan. 2012.
- [25] D. Thanou, E. Kokopoulou, Y. Pu, and P. Frossard, “Distributed average consensus with quantization refinement,” *IEEE Trans. Signal Process.*, vol. 61, no. 1, pp. 194–205, Jan. 2013.
- [26] S. Zhu, Y. C. Soh, and L. Xie, “Distributed parameter estimation with quantized communication via running average,” *IEEE Trans. Signal Process.*, vol. 63, no. 17, pp. 4634–4646, Sep. 2015.
- [27] M. El Chamie, J. Liu, and T. Başar, “Design and analysis of distributed averaging with quantized communication,” *IEEE Trans. Autom. Control*, vol. 61, no. 12, pp. 3870–3884, Dec. 2016.
- [28] H. Li, G. Chen, T. Huang, and Z. Dong, “High-performance consensus control in networked systems with limited bandwidth communication and time-varying directed topologies,” *IEEE Trans. Neural Netw. Learn. Syst.*, vol. 28, no. 5, pp. 1043–1054, May 2017.
- [29] C.-S. Lee, N. Michelusi, and G. Scutari, “Topology-agnostic average consensus in sensor networks with limited data rate,” in *Proc. 51st ACSSC*, Oct. 2017.
- [30] —, “Distributed quantized weight-balancing and average consensus over digraphs,” in *Proc. 57th IEEE CDC*, Dec. 2018.

- [31] C.-S. Lee, N. Michelusi, and G. Scutari, “Finite rate distributed weight-balancing and average consensus over digraphs,” *IEEE Trans. Autom. Control (Early Access)*, pp. 1–1, 2020.
- [32] D. Alistarh, D. Grubic, J. Li, R. Tomioka, and M. Vojnovic, “Qsgd: Communication-efficient sgd via gradient quantization and encoding,” in *Proc. 31st NeurIPS*, Dec. 2017.
- [33] D. Alistarh, T. Hoeffler, M. Johansson, N. Konstantinov, S. Khirirat, and C. Renggli, “The convergence of sparsified gradient methods,” in *Proc. 32nd NeurIPS*, Dec. 2018.
- [34] P. Karimireddy, Q. Rebjock, S. Stich, and M. Jaggi, “Error feedback fixes signsgd and other gradient compression schemes,” in *Proc. 36th ICML*, Jul. 2018.
- [35] S. U. Stich, J.-B. Cordonnier, and M. Jaggi, “Sparsified sgd with memory,” in *Proc. 32nd NeurIPS*, Dec. 2018.
- [36] A. Koloskova, S. U. Stich, and M. Jaggi, “Decentralized stochastic optimization and gossip algorithms with compressed communication,” in *Proc. 36th ICML*, Jun. 2019.
- [37] X. Zhang, J. Liu, Z. Zhu, and E. S. Bentley, “Compressed distributed gradient descent: Communication-efficient consensus over networks,” in *Proc. IEEE INFOCOM*, Apr. 2019, pp. 2431–2439.
- [38] S. Zheng, Z. Huang, and J. Kwok, “Communication-efficient distributed blockwise momentum sgd with error-feedback,” in *Proc. 33rd NeurIPS*, Dec. 2019.
- [39] E. Gorbunov, F. Hanzely, and P. Richtárik, “A unified theory of sgd: Variance reduction, sampling, quantization and coordinate descent,” in *Proc. 23rd AISTATS*, Apr. 2020.
- [40] S. U. Stich, “On communication compression for distributed optimization on heterogeneous data,” *arXiv:2009.02388v2*, Dec. 2020.
- [41] F. Haddadpour, M. M. Kamani, A. Mokhtari, and M. Mahdavi, “Federated learning with compression: Unified analysis and sharp guarantees,” in *Proc. 24th AISTATS*, Apr. 2021.
- [42] C. A. Uribe, S. Lee, A. Gasnikov, and A. Nedić, “A dual approach for optimal algorithms in distributed optimization over networks,” *Optimization Methods and Software*, vol. 36, no. 1, pp. 171–210, 2021.
- [43] W. Shi, Q. Ling, G. Wu, and W. Yin, “Extra: An exact first-order algorithm for decentralized consensus optimization,” *SIAM J. Optim.*, vol. 25, p. 944–966, May 2015.
- [44] J. Xu, S. Zhu, Y. C. Soh, and L. Xie, “Convergence of asynchronous distributed gradient methods over stochastic networks,” *IEEE Trans. Autom. Control*, vol. 63, no. 2, pp. 434–448, Feb. 2018.
- [45] A. Nedić, A. Olshevsky, and W. Shi, “Achieving geometric convergence for distributed optimization over time-varying graphs,” *SIAM J. Optim.*, vol. 27, no. 4, pp. 2597–2633, Dec. 2017.
- [46] G. Qu and N. Li, “Harnessing smoothness to accelerate distributed optimization,” *IEEE Trans. Control. Netw. Syst.*, vol. 5, no. 3, pp. 1245–1260, Sep. 2018.
- [47] J. Xu, Y. Tian, Y. Sun, and G. Scutari, “Distributed algorithms for composite optimization: Unified and tight convergence analysis,” *arXiv:2002.11534v2*, Mar. 2020.
- [48] J. Xu, S. Zhu, Y. C. Soh, and L. Xie, “Augmented distributed gradient methods for multi-agent optimization under uncoordinated constant stepsizes,” in *Proc. 54th IEEE CDC*, Dec. 2015, pp. 2055–2060.
- [49] Z. Li, W. Shi, and M. Yan, “A decentralized proximal-gradient method with network independent step-sizes and separated convergence rates,” *arXiv:1704.07807v2*, Jun. 2019.
- [50] K. Yuan, B. Ying, X. Zhao, and A. H. Sayed, “Exact diffusion for distributed optimization and learning—part i: Algorithm development,” *IEEE Trans. Signal Process.*, vol. 67, no. 3, pp. 708–723, Feb. 2019.
- [51] S. A. Alghunaim, E. Ryu, K. Yuan, and A. H. Sayed, “Decentralized proximal gradient algorithms with linear convergence rates,” *IEEE Trans. Autom. Control (Early Access)*, pp. 1–1, 2020.

- [52] A. Nedić and A. Ozdaglar, “Distributed subgradient methods for multi-agent optimization,” *IEEE Trans. Autom. Control*, vol. 54, no. 1, pp. 48–61, Jan. 2009.
- [53] D. P. Bertsekas and J. N. Tsitsiklis, *Parallel and Distributed Computation: Numerical Methods*. Belmont, MA, USA: Athena Scientific, 1989.
- [54] A. Agarwal, S. Negahban, and M. J. Wainwright, “Fast global convergence rates of gradient methods for high-dimensional statistical recovery,” in *Proc. 24th NeurIPS*, Dec. 2010, pp. 37–45.
- [55] L. Xiao and S. Boyd, “Fast linear iterations for distributed averaging,” *Syst. Contr. Lett.*, vol. 53, no. 1, pp. 65–78, 2004.
- [56] Y. Lecun, L. Bottou, Y. Bengio, and P. Haffner, “Gradient-based learning applied to document recognition,” *Proc. IEEE*, vol. 86, no. 11, pp. 2278–2324, Nov. 1998.
- [57] J. J. Moreau, “Proximité et dualité dans un espace hilbertien,” *Bulletin de la Société Mathématique de France*, vol. 93, pp. 273–299, 1965.
- [58] Y. Nesterov, *Introductory Lectures on Convex Optimization: A Basic Course*, 1st ed. Springer Publishing Company, Incorporated, 2014.